Entropy-Driven Phase Transitions in Complex Ceramic Oxides

R. Jackson Spurling[1,2], Eric A. Lass[1], Xin Wang[1], and Katharine Page[1,*]
[1]Materials Science and Engineering Department, University of Tennessee-Knoxville
[2]Department of Materials Science and Engineering, Pennsylvania State University

*Corresponding author: kpage10@utk.edu

ABSTRACT: The recent development of multicomponent, high-entropy oxides has sparked research into novel ceramics with significant compositional and structural diversity. The wide range of compositions and structures achievable with these high-entropy oxides presents a promising research opportunity, as these materials may be custom-designed to serve in any of a number of important applications, from chemical catalysis to lithium-ion batteries. Many of the unique properties which make these materials viable for a variety of applications are attributed to the characteristic single-phase structure of high-entropy oxides. As such, some of the research into high-entropy oxides to-date has focused on understanding the driving force which results in this transition from a multi-phase to a single-phase structure. The continued development of these materials relies on establishing a sound fundamental understanding of these critical phase transformations. To that end, this work will review the recent research advancements investigating phase transitions in high-entropy oxides. This review will leverage mathematical and empirical evidence to compare the effects of enthalpic and entropic contributions to the free energy of mixing and, in turn, their impact on the transition to single-phase high-entropy oxides. Particular emphasis will be placed on the role of entropy stabilization in these phase transitions as well as other property effects arising from high entropic lattice disorder.

Keywords: high-entropy oxides, phase transformations, entropic and enthalpic contributions

I. Introduction to High-Entropy Oxides

The pursuit of compositionally complex, versatile materials with tailorable properties has long served as a motivating factor for materials research and design. Recently, the development of high-entropy materials has attracted significant research interest. The concept of high-entropy materials was initially pioneered in 2004 independently by Yeh, *et al.*[1] and Cantor, *et al*[2]. While early research focused on high-entropy alloys, the work by Rost, *et al.*[3] in 2015 opened the door for novel research into high-entropy ceramics, and in particular high-entropy oxides (HEOs).

Rost, *et al.* were successful in demonstrating that a $(Co_{0.2}Cu_{0.2}Mg_{0.2}Ni_{0.2}Zn_{0.2})O$ multicomponent oxide could be synthesized and produces a single-phase at high temperatures[3]. Not only were the authors able to prove that such a structure is stable, but also that the transition from a multi-phase structure to a single-phase rocksalt structure is entropy-stabilized; that is, the single-phase transition is stabilized through the configurational entropy contribution derived from high cation sublattice disorder. The entropic and enthalpic contributions to the system free energy dictate phase transformation thermodynamics in HEOs[3–12]. Since this initial work by Rost, *et al.*[3], additional high-entropy ceramics‡ have been synthesized, particularly oxides[4–9,13–30]. Most of these studies have focused on synthesizing single-phase HEOs and moved directly to property characterization; however, some studies have extended to examining the role of entropy in stabilizing the single-phase structure[4–7]. These studies provide evidence of the thermodynamic contributions which govern the phase transformation behaviors and synthesis of single-phase HEOs.

This work will examine the existing literature in an effort to describe the thermodynamics of phase transformations in HEOs. Entropic and enthalpic contributions will be concisely defined and their role in the transition to single-phase HEOs will be examined. Additionally, experimental work will be examined to succinctly describe how phase transitions are studied in HEOs, including a discussion of how entropy-stabilization may be identified as the driving force for a given phase transformation.

II. Thermodynamics of Phase Transitions

II.I Configurational Entropy and Lattice Disorder

Given that the distinguishing feature of HEOs is the maximization of the configurational entropy (S_{conf}), it is most convenient to define this class of materials in these terms. In general, HEOs are taken to be multicomponent single-phase complex oxides having five or more constituent cations, resulting in a configurational entropy of $S_{conf} \geq 1.5R$, where R is the universal gas constant[10–12]. The ideal configurational entropy is expressed in Equation 1 as follows[3,10–12]:

$$S_{conf} = -R \sum_{i=1}^{N} x_i \, ln(x_i) \qquad Eq. 1$$

In the above equation, R is the universal gas constant, N is the number of components (in this case, the number of constituent cation types), and x_i is the atomic fraction of the i^{th} cation species. In Equation 1, we have neglected the contributions of configurational disorder on the anion sublattice; this assumption holds for HEOs due to the fact that there is only one anion species (i.e. oxygen) which is located regularly on lattice positions. Therefore, the S_{conf} of the system is due to lattice disorder amongst the cation species. We also assume that cation disorder is relegated to a single sublattice position; however, Equation 1 may be easily modified to account for multiple-site cationic sublattice disorder, such as for the A- and B-site sublattices in more complex oxides like perovskites[10].

There are two important trends that result from the mathematical description of the configurational entropy presented in Equation 1; that is, the entropy will increase with a higher number of constituent cations and will be maximized at equimolar cation ratios. Hence, HEOs are designed to have equimolar ratios of five or more cations in order to attain a high configurational entropy. This behavior of configurational entropy is illustrated graphically in Figure 1. By designing these oxides with 5+ equimolar components, the configurational entropy is raised to overcome enthalpic driving forces and stabilize a single-phase structure (see Section III.I).

‡For discussions on high-entropy ceramics beyond oxides and direction to relevant literature, please see the Appendix.

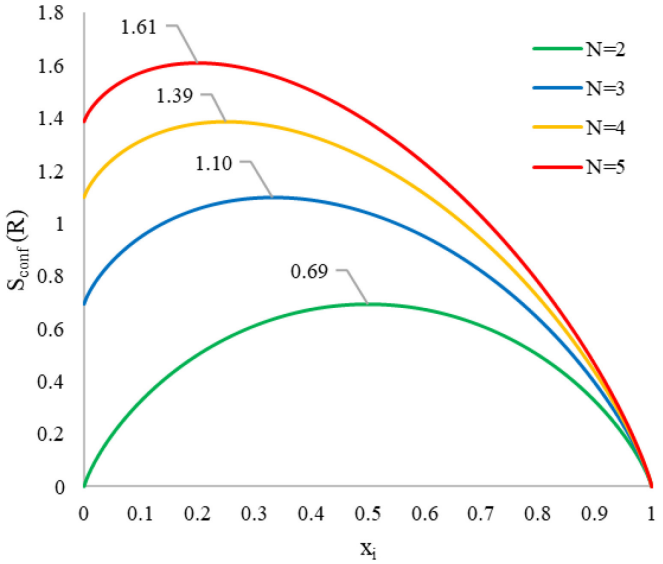

Figure 1. Configurational entropy varies as a function of both the number and mole fraction of components (i.e. constituent cations). For a given number of cations, the configurational entropy will be maximized at equimolar cation ratios.

II.II Entropic and Enthalpic Considerations

A fundamental tenant of thermodynamics as it relates to phase transformations is that the minimization of free energy serves as the driving force governing these phase transitions. The free energy of the system is defined in Equation 2 below:

$$\Delta G_{mix} = \Delta H_{mix} - T\Delta S_{mix} \qquad Eq. 2$$

Therefore, the transition from a multi-phase to a single-phase state (as required for these HEOs) must be favorable via a minimization of the free energy. In short, single-phase transformations in HEOs will occur when ΔG_{mix} becomes negative (i.e. the entropy term overpowers the positive enthalpy of formation of the single phase).

Considering the multi-to-single-phase transition in HEOs, we may define two opposing thermodynamic driving forces. As discussed in the previous subsection, the configurational entropy is maximized for equimolar cation ratios and increases with the addition of constituent cations. This entropy term is in competition with the enthalpic driving force, which resists the formation of a single-phase structure.

To form a single phase, the constituent oxides must arrange onto a single lattice. Not all of the constituent oxides necessarily exist in the same initial lattice configuration (and those that do will typically have disparate lattice constants); therefore, a transformation to a single-phase with a single (average) lattice constant must occur, the energy requirement for which is encompassed by the ΔH_{mix} term of Equation 2. This phase formation enthalpy requirement $(\Delta H^{\alpha\rightarrow\beta})$ can be considered an energy penalty working against the entropic driving force, promoting phase segregation.

From Equation 2, it is also evident that the ΔS_{mix} term is temperature-dependent; therefore, at a sufficient temperature, it is possible for the entropic driving force to overcome the enthalpic energy penalty (that is, $\Delta G_{mix}<0$), resulting in the formation of a single-phase solid solution. The importance of entropy in driving the transition to a single phase has led to the creation of a classification of compositionally complex oxides distinct from HEOs: entropy-stabilized oxides (ESOs)[3,7,10].

It is important to clarify the differences between the general class of high-entropy oxides and the specific class of entropy-stabilized oxides[10]. The former classification refers to all single-phase, multicomponent complex oxides, systems ($N_{cations} \geq 5$) satisfying the previously stated requirement, $S_{conf} \geq 1.5R$. As a result of this high configurational entropy, HEOs generally experience entropic property effects (discussed in greater detail in Section VII). ESOs, on the other hand, possess a stable single-phase structure directly due to the dominance of the entropic driving force during the phase transformation. While all HEOs do possess a high configurational entropy, depending upon the system, this entropy may not be sufficient (or, in the case of $\Delta H_{mix} < 0$, not needed) to overcome the high enthalpy of formation for the single phase, and thus the system may not be a true ESO.

A number of studies have conclusively demonstrated the dominance of high entropy in driving the formation of a single phase[3–7]. However, other studies have noted that, while entropy does play a role in stabilizing some single-phase HEOs, the configurational entropy may not always overcome the enthalpy of the phase transformation, resulting in intermediate phase formation[10–12]. The latter case represents a situation where enthalpy dominates in Equation 2.

This competition between entropic and enthalpic components in the single-phase transformation in HEOs as predicted by thermodynamics presents an important research question: What experimental evidence is there for entropy-stabilization of single-phase HEOs? To address this fundamental question, the remainder of this work will focus on the experimental approaches used to confirm the presence of single-phase HEOs and identify the driving forces responsible for the phase transformation. We will present a variety of different characterization methods as tools for assessing the thermodynamic behavior of these phase transformations and will offer a perspective on the outlook of these studies.

III. Single Phases in High-Entropy Oxides

III.I Structure of High-Entropy Oxides

HEOs are characterized by high levels of lattice disorder, resulting from their high configurational entropy. In high-entropy ceramics, as with traditional ionic crystals, the structure can be viewed as cations occupying particular interstitial vacancies within close-packed anion arrays (e.g. oxygen). However, in HEOs, unique cation species are not regularly ordered on interstitial positions; rather, they are randomly dispersed on these cation positions throughout the lattice, forming a relatively uniform distribution. Assuming that complete cationic sublattice disorder is achieved, with neither long- nor short-range ordering of cations (see Section VI), then a true single-phase material is achieved. This characteristic structural arrangement of HEOs is illustrated in Figure 2. HEO single-phase materials have been shown to crystallize in a variety of different structural configurations, including the rocksalt[3], perovskite[4,5], and fluorite[6,7] systems. In each case, a homogenous dispersion of cations and the absence of secondary phases qualifies the system as existing as a single-phase material.

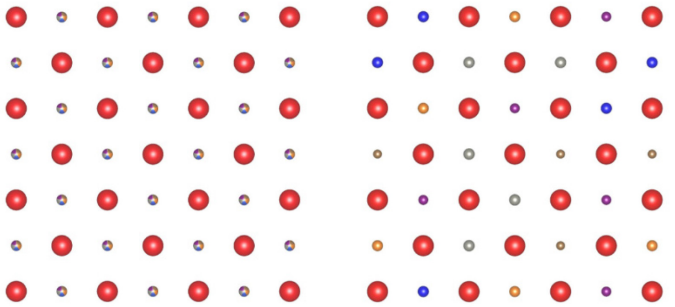

Figure 2. Schematic representation of a 3 x 3 unit cell array of a sample (100) family plane of a hypothetical single-phase rocksalt five-component HEO. Oxygen anions are represented by red spheres, while the smaller colored spheres represent atoms featuring an average site occupancy of five cation species (left) and the real randomized site occupancy (right). Note that these oxides tend to be ionically bonded species. The highly disordered cation sublattice is a manifestation of the system's high configurational entropy.

III.II Experimental Observations of Single Phases

Before experimentally examining the thermodynamic driving forces behind an HEO multi-to-single-phase transformation, it is first necessary to confirm the existence of a single phase. There are a variety of ways that this may be accomplished, although two routes are most prominently utilized in the literature: X-ray diffraction (XRD) and energy dispersive X-ray spectroscopy (EDXS).

The formation of a single-phase HEO may be confirmed by observing the temperature-dependent evolution of the XRD pattern. Initially, the constituent oxides exist independently, possessing their own unique structures. In the case of the work by Rost, *et al*[3], MgO, CoO, and NiO exist as rocksalt structures, while CuO and ZnO exist as tenorite and wurtzite structures, respectively. The initial presence of these secondary phases can be confirmed through XRD (Figure 3). As temperature increases, the enthalpy resisting the transition of CuO and ZnO into a rocksalt single-phase lattice is eventually overcome by the $T\Delta S_{mix}$ term, leading to the disappearance of the diffraction peaks attributed to the secondary phases and the formation of a single-phase solid solution. This temperature-dependent evolution of the diffraction pattern can be observed through X-ray diffraction, as demonstrated in Figure 3. The dominance of a single set of peaks and the absence of any secondary peaks at high temperatures is evidence that a single-phase HEO was successfully produced.

There are key experimental challenges that are little discussed in present literature when it comes to establishing a single-phase ESO with XRD methods. These include simple phenomena, such as the difficulty of detecting small impurity peaks given the fluorescence effects many transition metals experience under laboratory XRD radiation, and more complex phenomena, such as peak shape effects from strain and particle morphology, and peak intensity effects from crystallographic texture or cation sublattice order/disorder. A challenge of specific importance to the field of HEOs and ESOs is separating the effects of overlapped reflections due to symmetry lowering from those of multiple, similar phases. Such tasks are exceptionally challenging for structure types that intrinsically feature many closely spaced or overlapped Bragg peaks. We note that a subset of HEO literature to date includes full-profile Rietveld refinements, which are key when quantitatively distinguishing such factors with powder diffraction data. We bring attention to a variety of examples in Figure 4 germane to the determination of phase-purity and compositional homogeneity in complex oxides, HEOs, or ESOs via X-ray or neutron powder diffraction studies.

Figure 4a displays results of a combined Rietveld refinement of high-resolution synchrotron powder X-ray diffraction patterns and neutron powder diffraction patterns for the commensurately modulated highly disordered oxide $Zr_6Ta_2O_{17}$ (space group: *Ima2*, #46)[31]. The analysis

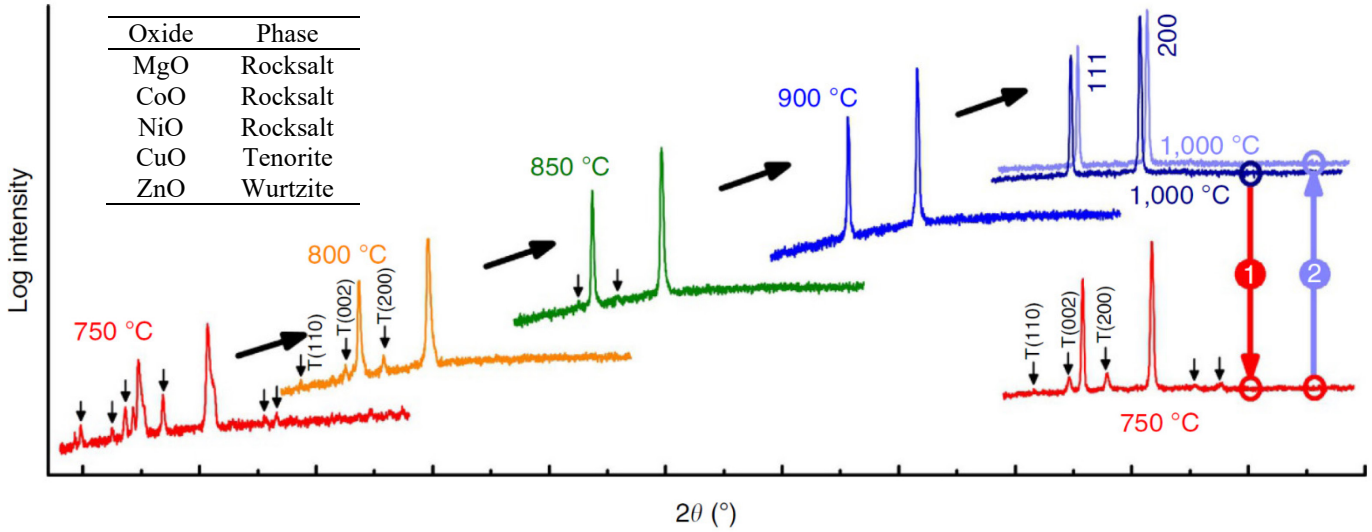

Figure 3. XRD patterns of a $(Co_{0.2}Cu_{0.2}Mg_{0.2}Ni_{0.2}Zn_{0.2})O$ rocksalt HEO are shown above. The patterns were collected after 2-hour equilibration at the specified temperature and subsequent air quenching. As temperature increases, the secondary phases (notated by small arrows) are observed to disappear, ultimately leading to the formation of a single-phase solid solution in the rocksalt structure. The tablular insert identifies the parent phase of each constituent oxide. Reproduced from Rost, et al[3].

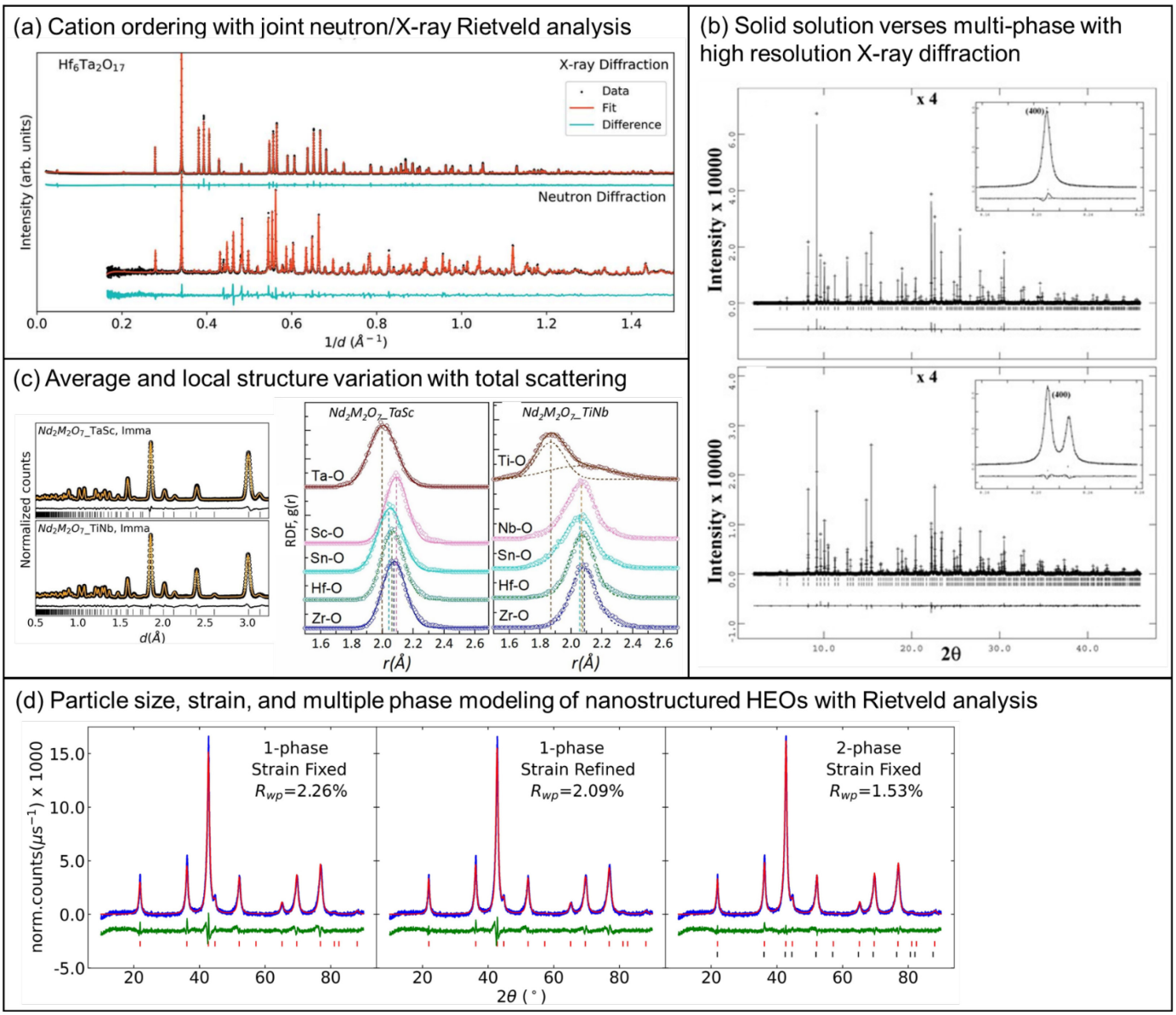

Figure 4. A montage of analyses pertinent to distinguishing the attainment of phase-purity and compositional homogeneity in complex oxides, HEOs, and ESOs via X-ray or neutron powder diffraction studies: (a) Synchrotron X-ray and neutron powder diffraction patterns, and Rietveld refinement, verifying single phase for the commensurately modulated and cation disordered $Zr_6Ta_2O_{17}$[31] (b) High resolution synchrotron X-ray diffraction patterns and Rietveld analysis distinguishing a single-phase garnet solid solution sample with average composition $[Mg_{2.30}Fe^{2+}_{0.26}Ca_{0.42}Mn^{2+}_{0.02}]_3[Al_{1.53}Fe^{3+}_{0.06}Cr^{3+}_{0.40}Ti_{0.01}Fe^{2+}_{0.01}]_2Si_3O_{12}$ (top panel) from a multi-phase sample with average composition $[Mg_{2.33}Fe^{2+}_{0.33}Ca_{0.33}Mn^{2+}_{0.01}]_3[Al_{1.73}Fe^{3+}_{0.12}Cr^{3+}_{0.06}Ti_{0.05}Fe^{2+}_{0.05}]_2Si_3O_{12}$ (bottom panel)[33]; (c) Neutron diffraction (left) and neutron PDF (right) analysis uncovering variation in the local bonding environments of the closely related orthorhombic pyrochlore HEO compositions $Nd_2(Ta_{0.2}Sc_{0.2}Sn_{0.2}Hf_{0.2}Zr_{0.2})_2O_7$ (labelled $Nd_2M_2O_7$_TaSc) and $Nd_2(Ti_{0.2}Nb_{0.2}Sn_{0.2}Hf_{0.2}Zr_{0.2})_2O_7$ (labelled $Nd_2M_2O_7$_TiNb)[37]; and (d) Rietveld refinement of an X-ray diffraction pattern of a nanostructured spinel sample with average composition of $(Mn_{0.2}Fe_{0.2}Ni_{0.2}Mg_{0.2}Cu_{0.2})Co_2O_4$, fit with a single phase model and crystalline grain size broadening (left panel), a single phase model incorporating strain broadening (middle panel), and a model containing two spinel phases that differ only in their phase fraction and cubic lattice parameter (right panel). See text for further discussion.

demonstrates a phase pure sample, where X-ray diffraction is used to obtain accurate cation positions and neutron diffraction is used to obtain accurate oxygen positions, due to their complementary scattering sensitivities. The strongly contrasting X-ray scattering factors for Zr and Ta additionally confirm the presence of severe cation disorder; cation disorder is important in the $A_6B_2O_{17}$ (A = Zr, Hf; B = Nb, Ta) family[32].

A sample that appears X-ray phase pure at first glance from peak indexing can be difficult to distinguish from one composed of several distinct but similar phases (with closely overlapping *hkl* reflections). In such a case, the Bragg peaks of distinct phases may overlap significantly and not be recognized as a multi-phase structure. While it was not directly discussed

in the original work[3], this effect is likely on display in Figure 3, where the Bragg peaks for the 800 °C, 850 °C, and 900 °C rock salt phase appear asymmetric and broadened compared to those observed upon and after annealing at 1000 °C. Multiple and closely related phases can often be identified by a full profile least-squares refinement of powder diffraction data (Rietveld analysis). It may prove necessary to collect high resolution data from a monochromatic source and/or expand a data collection window to include higher *d*-spacing peaks in such an endeavor. Such requirements have been noted in distinguishing single phase solid solutions from distinct but closely related multi-phases in garnet, spinel, and other complex oxides[33–36]. A demonstration is given in Figure 4b for two complex garnet minerals; the $[Mg_{2.30}Fe^{2+}_{0.26}Ca_{0.42}Mn^{2+}_{0.02}]_3[Al_{1.53}Fe^{3+}_{0.06}Cr^{3+}_{0.40}Ti_{0.01}Fe^{2+}_{0.01}]_2Si_3O_{12}$ sample in the top panel is confirmed as a single-phase solid solution, while the sample in the bottom panel is demonstrated to be a multi-phase compound with an average composition of $[Mg_{2.33}Fe^{2+}_{0.33}Ca_{0.33}Mn^{2+}_{0.01}]_3[Al_{1.73}Fe^{3+}_{0.12}Cr^{3+}_{0.06}Ti_{0.05}Fe^{2+}_{0.05}]_2Si_3O_{12}$ (this sample has less Cr^{3+} and more Al^{3+} cations in the octahedral site and exhibits birefringence from the strain experienced by the secondary, minor phase)[33]. Very few reported HEOs have been studied with high resolution diffraction, and thus the extent to which such effects may be present among them has not yet been carefully examined.

Even in cases where the average structure as modeled by Rietveld refinement indicates a single phase, studies of the local atomic structure may reveal significant distortions of local environments, variations in chemical short-range order (CSRO), or the presence of multiple different nanostructured regions[30,37–39]. Figure 4c displays partial results of a detailed atomic structure analysis of two closely related HEO pyrochlore structures, $Nd_2(Ta_{0.2}Sc_{0.2}Sn_{0.2}Hf_{0.2}Zr_{0.2})_2O_7$ (labelled $Nd_2M_2O_7$_TaSc) and $Nd_2(Ti_{0.2}Nb_{0.2}Sn_{0.2}Hf_{0.2}Zr_{0.2})_2O_7$ (labelled $Nd_2M_2O_7$_TiNb)[37]. Neutron diffraction analysis, shown on the left, indicates a phase pure orthorhombic pyrochlore structure (spacegroup: *Imma*, #74) for both samples. However, the result of Reverse Monte Carlo neutron diffraction and pair distribution functional analysis on the right, supported by Density Functional Theory, Molecular Dynamics simulations, and Metropolis Monte Carlo simulations, reveals that the $Nd_2M_2O_7$_TaSc composition is synthesized with its M-site local to microscopic order highly randomized/disordered, while the $Nd_2M_2O_7$_TiNb composition displays a strong local distortion of TiO_6 octahedra. Note that the presence of local lattice distortions or CSRO does not constitute a new phase unless it is seen to grow in size given time and thermal energy. In fact some degree of disorder exists in all materials where the enthalpy of mixing is non-zero, even in a single-phase, entropy stabilized material. The extent to which differing degrees of CSRO and local atomic distortions are prevalent among HEOs and ESOs deserves further study.

Verifying the attainment of a single phase with XRD may require sorting out the origin of specimen broadening effects in observed X-ray or neutron powder diffraction patterns, which requires careful modeling of instrument profile functions. The task is even more challenging in nanostructured HEOs, where finite crystalline grain size, strain broadening effects, and low signal to noise ratios may be present in diffraction data. A significant portion of HEO literature to date contains diffraction data with visibly asymmetric and/or broadened peak shapes[30,40–44]. Sometimes these effects are discussed and modeled and sometimes they are not. Such instances may indicate the presence of significant strain, a lower symmetry structure, multiple closely related (secondary) phases, a compositional gradient, or other effects. A demonstration is shown from our own work in Figure 4d for a nanostructured spinel oxide with average composition $(Mn_{0.2}Fe_{0.2}Ni_{0.2}Mg_{0.2}Cu_{0.2})Co_2O_4$, where it is seen in the resulting difference curve that Bragg peak features are not well-fit with a single phase spinel structure model with spherical particle size broadening (left panel, R_{wp} = 2.26%). The addition of a strain parameter (middle panel, R_{wp} = 2.09%) does little to improve the fit, but a 2-phase spinel structure model incorporating separately refined cubic lattice parameters (right panel, R_{wp} = 1.53%) provides a significantly improved result. Note this is not sufficient evidence to confirm a multi-phase nanostructured oxide; a model with three phases and three lattice parameters would provide an even better fit to data. This peak asymmetry could be caused by a composition gradient resulting from the dissolution of two isostructural phases with different compositions dissolving in one another to form a single phase. If this nanostructured oxide is a multi-phase spinel with overlapping Bragg peaks, rather than a true solid solution, it will possess multiple distinct regions with distinct compositions and lattice parameters. This also means it will likely feature fewer cations in each of its separate phases and less overall entropy stability, and thus may not qualify as a HEO as defined in this review. How phase purity is characterized and even defined in HEO systems and what structural analysis will ultimately be necessary to understand their key physical properties are evolving topics.

In contrast to XRD, EDXS offers a more qualitative method for confirming the existence of a single-phase HEO. As described in Section II.I, cationic sublattice disorder is an embodiment of the high configurational entropy that is characteristic of HEOs. The random, homogenous distribution of the cations throughout the HEO structure is a requirement for the formation of the single-phase structure. Therefore, proof of long-range, uniform dispersion of the cations in the sample structure would consequently serve as evidence of a single-phase. This is conventionally accomplished via EDXS mapping, which is a common feature of most standard EDXS detectors. EDXS maps can show the relative distribution of the atoms (in this case, cations) within the sample structure. Provided that a large enough area of the sample surface is mapped, it is not usually necessary to perform quantitative analysis with this form of EDXS; when paired with XRD, it is generally sufficient to use EDXS to show the homogenous distribution of cations.

Alternate (and generally more quantitative and intensive) methods for establishing a high degree of cation disorder and therefore chemical homogeneity in HEOs have included atom probe tomography (APT), X-ray absorption fine structure (EXAFS), X-ray absorption near edge spectroscopy (XANES) and X-ray magnetic circular dichroism (XMCD), X-ray or neutron diffraction and pair distribution function (PDF), atomic force microscopy (AFM), neutron spectroscopy,

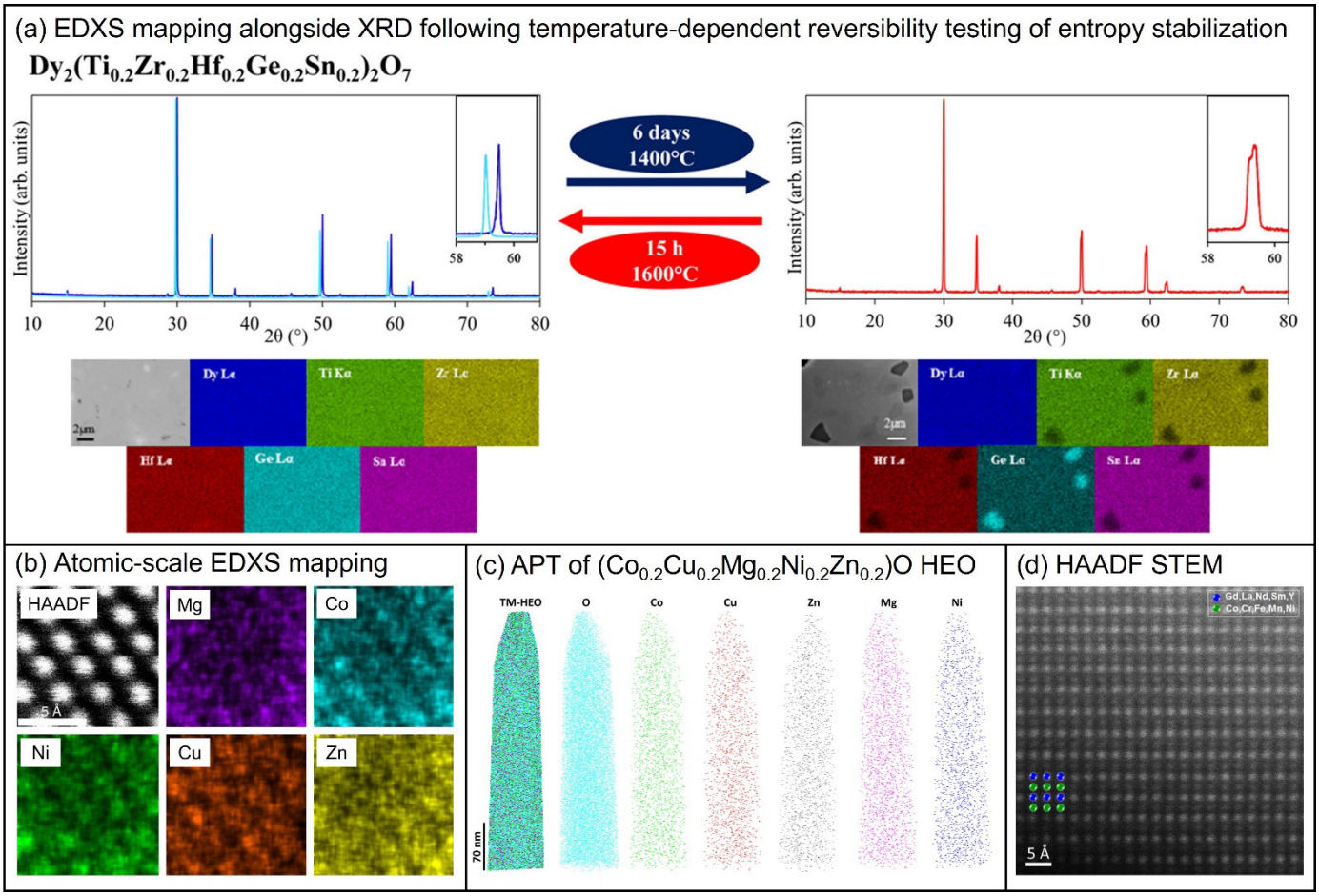

Figure 5. A montage of examples of methods for chemical homogeneity studies in HEOs. (a) The transition to single-phase pyrochlore $Dy_2(Ti_{0.2}Zr_{0.2}Hf_{0.2}Ge_{0.2}Sn_{0.2})_2O_7$ is shown to be temperature-dependent and reversible from XRD, with accompanying EDXS mapping showing clear precipitation of a Ge-rich secondary phase[8]. (b) Atomic scale EDXS mapping of uniform cation distributions in $(Co_{0.2}Cu_{0.2}Mg_{0.2}Ni_{0.2}Zn_{0.2})O$ rocksalt HEO[3]. (c) Atom-probe tomography maps of the $(Co_{0.2}Cu_{0.2}Mg_{0.2}Ni_{0.2}Zn_{0.2})O$ HEO likewise show homogeneity in the cation distribution[47]. (d) A high-angle annular dark field (HAADF) scanning transmission electron micrograph shows ordering of cation columns in the $(Gd_{0.2}La_{0.2}Nd_{0.2}Sm_{0.2}Y_{0.2})(Co_{0.2}Cr_{0.2}Fe_{0.2}Mn_{0.2}Ni_{0.2})O_3$ HEO[5].

SQUID magnetometry, Mössbauer spectroscopy, Raman spectroscopy, electron paramagnetic resonance (EPR), and nuclear magnetic resonance (NMR) studies (see Section VI for further discussion)[45,46]. Collectively, these methods may be used to assess relative cation distributions and probe local coordination environments, which are critical in the study of HEOs; a number of reports exist in the literature which serve as excellent examples of the broad range of characterization techniques available for exploring cation distribution and local structures in HEOs[3,5,8,47,48]. Figure 5 provides examples of how a variety of different characterization techniques have been employed in the study of high-entropy oxides to probe chemical homogeneity.

IV. Entropic Phase Transformations

IV.I Entropy-Stabilized Oxides

As we have shown, thermodynamics predicts that the entropic driving force may stabilize the formation of single-phase HEOs when sufficient temperature is reached to overcome the enthalpic energy penalty associated with the transition from an equilibrium multi-phase to an equilibrium single-phase. Rost, *et al.* demonstrated that the single-phase structure of the $(Co_{0.2}Cu_{0.2}Mg_{0.2}Ni_{0.2}Zn_{0.2})O$ HEO was entropy-stabilized through a series of three corroborating observations of the phase transformation: temperature-dependent reversibility, endothermicity, and component addition[3].

While most studies have focused on maximizing a system's configurational entropy, it is important to note that the system need only overcome the enthalpic resistance to the phase transformation, meaning that the entropy threshold for such a transformation varies by system. In the case of the canonical $(Co_{0.2}Cu_{0.2}Mg_{0.2}Ni_{0.2}Zn_{0.2})O$ HEO, the configurational entropy is in competition with the enthalpy of formation which serves as a barrier to the transition of ZnO and CuO into the rocksalt single-phase from the original wurtzite and tenorite structures. Therefore, entropy-stabilization under an ideal solution assumption would require these enthalpic penalties to be overcome, which must be a temperature-dependent phenomenon. Moreover, measuring the directional heat flow can also demonstrate the endothermicity of the transformation, thus providing a second route for testing entropy-stabilization. Finally, removing components would lower the configurational entropy of the system, and therefore component addition may be used to assess if the entropic threshold for single-phase stabilization is met. Thus, three clear methods arise for testing

the role of entropy in stabilizing the single-phase transformation.

Since this initial illustration of entropy-stabilization of HEOs by Rost, *et al.*, other groups have leveraged similar approaches to conclusively prove the role of entropy in stabilizing the single-phase transformation in novel HEOs[4–9]. Table 1 provides a survey of the literature of many reported single-phase HEO systems, with particular attention paid to those systems shown experimentally to be entropy-stabilized (including experimental approaches). Note that, while many single-phase HEOs have been produced, relatively few have been conclusively shown to be entropy stabilized.

Here, we have briefly established the foundation for each of three methods for testing entropy-stabilization, using the $(Co_{0.2}Cu_{0.2}Mg_{0.2}Ni_{0.2}Zn_{0.2})O$ rocksalt HEO as an example. The remainder of this section is devoted to examining the experimental approaches which have yielded evidence of true entropy-stabilized oxides, including the characterization techniques used and the systems studied.

IV.II Temperature-Dependent Reversibility

Thermal cycling takes advantage of the temperature dependence of the entropy term in the expression of the system free energy (Equation 1) to prove entropic stabilization of the HEO single-phase. Due to the temperature-dependence of this ΔS_{mix} term, it follows that there is a critical temperature for which $\Delta G = 0$; that is, the magnitude of $-T\Delta S_{mix}$ is equivalent to the magnitude of ΔH_{mix}. While at points above this temperature the single-phase may be entropy-stabilized, the system will exist as a multi-phase structure below this critical temperature. If the system is a true ESO, then the phase structure should be fully reversible by transiting this temperature boundary.

This temperature-dependent reversibility of the single-phase transformation has been leveraged most frequently by literature as a route to demonstrate the role of entropy-stabilization[3,5–9]. This is accomplished by allowing the system to equilibrate at a temperature at which the single phase is stable, with single-phase stability confirmed by XRD. Following this, equilibration at a lower temperature (below the critical temperature, $\Delta G(T_C) = 0$) is conducted, and the sample is again quenched and examined via XRD. As a result of the equilibration at lower temperature, the $-T\Delta S_{mix}$ decreases in value and is unable to overcome the enthalpic energy penalty to form a single phase; as a result, we expect the precipitation of one or more secondary phases, which is confirmed by comparing the XRD patterns at the low and high temperatures. An example of this process is shown in the right of Figure 3, as equilibration of the $(Co_{0.2}Cu_{0.2}Mg_{0.2}Ni_{0.2}Zn_{0.2})O$ HEO at 750 °C leads to formation of secondary phases, but subsequent equilibration at 1000 °C permits the re-formation of the rocksalt single phase[3]. Alternating multi-phase and single-phase formation as a result of repeated thermal cycling between these temperatures successfully demonstrates the temperature-dependent reversibility of the phase transformation, and consequently the role of entropy as the stabilizing driving force. As mentioned previously, this method can be more difficult to apply when the end member components are all stable in the same structure type (if the diffraction peaks of the separate phases closely overlap). In this latter case, Rietveld refinement or peak width analysis can be applied to HEO lattice reflections to demonstrate a transition from multiple overlapping peak contributions to single peak contributions.

IV.III Endothermicity

Another consequence of an entropy-stabilized single-phase transformation is that it must be endothermic. This transformation requires the influx of heat to overcome the enthalpy resisting the phase transformation, which can be measured directly via differential scanning calorimetry (DSC)[3]. The location of the endothermic peak in the DSC spectrum can be used to locate the single-phase transition temperature. Coupling the DSC data with XRD can provide

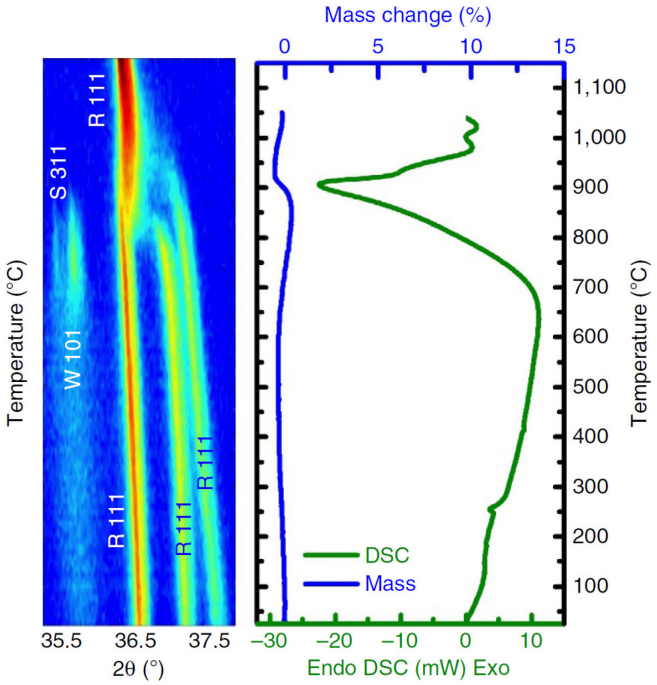

Figure 6. High-temperature in situ XRD (left) and DSC (right) were conducted for the $(Co_{0.2}Cu_{0.2}Mg_{0.2}Ni_{0.2}Zn_{0.2})O$ rocksalt HEO to prove the entropy-stabilization of the phase transformation and pinpoint the phase transition temperature via the observation of an endothermic peak corresponding to the emergence of a single-phase rocksalt structure. Reproduced from Rost, et al[3].

significant insight into the phase transformation, as high-temperature *in situ* X-ray diffraction can show the formation of a single set of diffraction peaks (and the disappearance of secondary peaks) concurrent with the endothermic peak of the DSC curve (Figure 6).

To-date, there are relatively few examples in the literature of calorimetry applied specifically to entropy-stabilized oxides (as a general rule, it appears that most studies have employed temperature-dependent reversibility over calorimetry methods for exploring entropy-stabilization). However, there are reports of other calorimetry techniques which have been used successfully in studies of compositionally complex and highly disordered oxides, such as oxide melt solution calorimetry[32]. Further reading on high-temperature calorimetry techniques and applications can be found in the literature[49].

Single-Phase Structure (Compositions)	S_{conf} Stability?	Experimental	References
Rocksalt (MO)			
$(Co_{0.2}Cu_{0.2}Mg_{0.2}Ni_{0.2}Zn_{0.2})O$	Yes	All Three Methods	[3,17,27,28]
*Other derivatives in the system, particularly Gd, Li, Na, K, and other dopants			
$(Mg_{0.33}Co_{0.33}Ni_{0.33})_{1-\delta}Zn_{\delta}O$	Yes	Reversibility	[9]
Fluorite (MO_2)			
$(Ce_{0.2}Zr_{0.2}Hf_{0.2}Sn_{0.2}Ti_{0.2})O_2$	Yes	Reversibility	[6]
$(Ce_{0.2}Zr_{0.2}Y_{0.2}Gd_{0.2}La_{0.2})O_{2-\delta}$	Yes	Reversibility	[7]
$(Hf_{0.25}Zr_{0.25}Ce_{0.25}Y_{0.25})O_{2-\delta}$	No	N/A	[16]
$(Hf_{0.25}Zr_{0.25}Ce_{0.25})(Y_{0.125}\Omega_{0.125})O_{2-\delta}$ *(Ω = Yb,Ca,Gd)	No	N/A	[16]
$(Hf_{0.25}Zr_{0.25}Ce_{0.25})(Yb_{0.125}Gd_{0.125})O_{2-\delta}$	No	N/A	[16]
$(Hf_{0.2}Zr_{0.2}Ce_{0.2})(Y_{0.2}\Omega_{0.2})O_{2-\delta}$ *(Ω = Yb,Gd)	No	N/A	[16]
$(Hf_{0.2}Zr_{0.2}Ce_{0.2})(Yb_{0.2}Gd_{0.2})O_{2-\delta}$	No	N/A	[16]
$(Ce_{0.2}La_{0.2}Sm_{0.2}Pr_{0.2}Y_{0.2})O_{2-\delta}$	No	N/A	[25]
Perovskite (ABO_3)			
$Sr(Zr_{0.2}Sn_{0.2}Ti_{0.2}Hf_{0.2}\Omega_{0.2})O_3$ *(Ω = Mn,Nb)	Yes	Component Addition	[4]
$Ba(Zr_{0.2}Sn_{0.2}Ti_{0.2}Hf_{0.2}\Omega_{0.2})O_3$ *(Ω = Nb,Ce,Y,Ta)	No	N/A	[4,26,29]
$(Sr_{0.5}Ba_{0.5})(Zr_{0.2}Sn_{0.2}Ti_{0.2}Hf_{0.2}Nb_{0.2})O_3$	No	N/A	[4]
$(Gd_{0.2}La_{0.2}Nd_{0.2}Sm_{0.2}Y_{0.2})MnO_3$	Yes	Reversibility	[5]
$(Gd_{0.2}La_{0.2}Nd_{0.2}Sm_{0.2}Y_{0.2})\Omega O_3$ *(Ω = Co,Fe)	No	N/A	[5]
$\Omega(Co_{0.2}Cr_{0.2}Fe_{0.2}Mn_{0.2}Ni_{0.2})O_3$ *(Ω = Gd,La,Nd)	No	N/A	[5]
$(Gd_{0.2}La_{0.2}Nd_{0.2}Sm_{0.2}Y_{0.2})(Co_{0.2}Cr_{0.2}Fe_{0.2}Mn_{0.2}Ni_{0.2})O_3$	No	N/A	[5]
Spinel (AB_2O_4)			
$(Co_{0.2}Cr_{0.2}Fe_{0.2}Mn_{0.2}\Omega_{0.2})_3O_4$ *(Ω = Ni,Mg,Zn)	No	N/A	[13,14,18,19]
$(Ni_{0.2}Cr_{0.2}Fe_{0.2}Mn_{0.2}\Omega_{0.2})_3O_4$ *(Ω = Mg,Zn)	No	N/A	[14,19]
$(Mg_{0.2}Co_{0.2}Ni_{0.2}Cu_{0.2}\Omega_{0.2})Fe_2O_4$ *(Ω = Fe,Zn)	No	N/A	[18]
$(Mn_{0.2}Co_{0.2}Ni_{0.2}Cu_{0.2}\Omega_{0.2})Fe_2O_4$ *(Ω = Fe,Mg)	No	N/A	[18]
$(Mg_{0.2}Co_{0.2}Ni_{0.2}Cu_{0.2}\Omega_{0.2})Cr_2O_4$ *(Ω = Fe,Zn,Mn)	No	N/A	[18]
$(Mg_{0.2}Co_{0.2}Ni_{0.2}Cu_{0.2}Zn_{0.2})Al_2O_4$	No	N/A	[18]
$(Al_{0.167}Co_{0.167}Cr_{0.167}Fe_{0.167}Mn_{0.167}Ni_{0.167})_3O_4$	No	N/A	[24]
Bixbyite ($(A,B)_2O_3$)			
$(Gd_{0.4}Tb_{0.4}Dy_{0.4}Ho_{0.4}Er_{0.4})O_3$	No	N/A	[15]
Pyrocholore ($A_2B_2O_7$)			
$(Gd_{0.2}Eu_{0.2}Sm_{0.2}Nd_{0.2}La_{0.2})_2Zr_2O_7$	No	N/A	[20]
$Dy_2(Ti_{0.2}Zr_{0.2}Hf_{0.2}Ge_{0.2}Sn_{0.2})_2O_7$	Yes	Reversibility	[8]
$(Eu_{0.2}Gd_{0.2}Dy_{0.2}Ho_{0.2}\Omega_{0.2})_2Zr_2O_7$ *(Ω = La,Sc,Tb)	No	N/A	[30]
$Y_2(TiZrHfMoV)_2O_7$	No	N/A	[22]
$Y_2(TiHfMo\Omega)_2O_7$ *(Ω = V,Zr)	No	N/A	[22]
$(Eu_{0.5}Gd_{0.5})_2(Ti_{0.33}Zr_{0.33}Sn_{0.33})_2O_7$	No	N/A	[21]
*Other derivatives in this system			
Magnetoplumbite ($AB_{12}O_{19}$)			
$Ba(Fe_6Ti_{1.2}Co_{1.2}In_{1.2}Ga_{1.2}Cr_{1.2})O_{19}$	No	N/A	[23]

Table 1. A survey of many of the single-phase HEOs reported in the literature, with particular emphasis placed on those reports of entropy stabilization. Additional lists of HEO compositions may be found in the literature[10,11,45,46].

IV.IV Component Addition

A third method to conclusively demonstrate the role of entropy in stabilizing the formation of a single-phase HEO is the removal or addition of components with a positive mixing enthalpy contribution. Referring to Equation 1, it may be seen that the addition of components will increase the configurational entropy. Therefore, changing the number of components should have a substantial impact on the system entropy, and in some cases force the stabilization of the single-phase. This effect is illustrated through the following hypothetical example: consider an equimolar, four-component, medium-entropy system ($S_{conf} = 1.39R$). If a fifth component is added, the ideal system configurational entropy is increased ($S_{conf} = 1.61R$). The entropy gain associated with this component addition may be sufficient to drive the single-phase formation. Therefore, this method presents compelling evidence of a true entropy-stabilized oxide via the entropy gain associated with component addition from a medium-entropy to a high-entropy oxide.

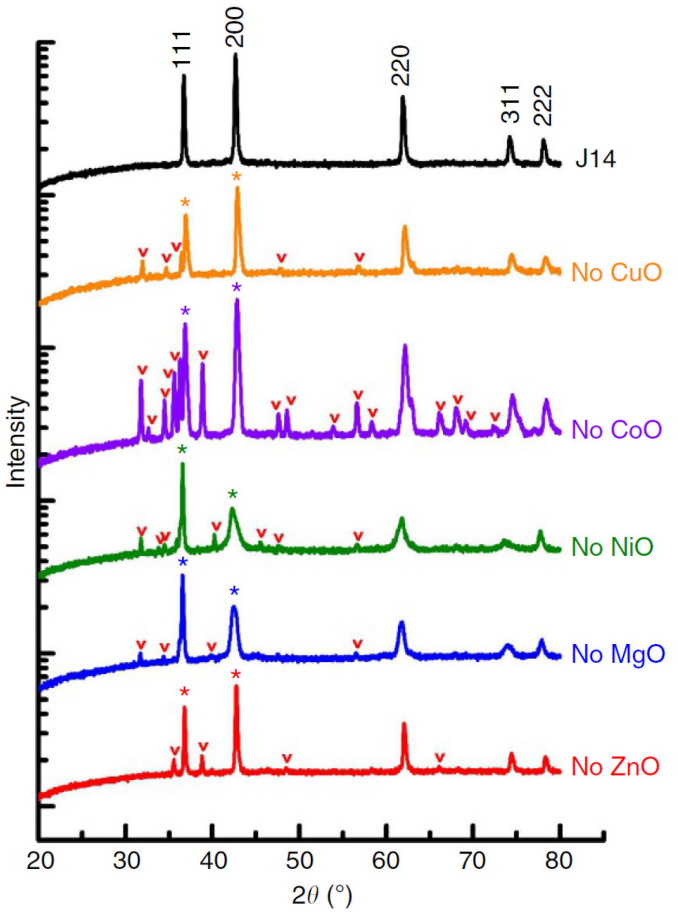

Figure 7. The XRD pattern of the complex oxide J14 represents the composition ($Co_{0.2}Cu_{0.2}Mg_{0.2}Ni_{0.2}Zn_{0.2}$)O equilibrated at high temperatures and exists in the single-phase rocksalt structure. The five subsequent XRD patterns are of the complex oxide with one of the constituents removed with an anneal for 12 hours at the observed single-phase transition temperature of 875 °C. In each case, the removal of a constituent oxide lowers the system configurational entropy enough that the single-phase structure is no longer stable at the original transition temperature, as demonstrated by the emergence of secondary diffraction peaks (noted by carrots). Therefore, this method demonstrates entropy stabilization. Reproduced from Rost, et al[3].

This approach has been employed with success in previous work[3,4]. In the rocksalt system, Rost, *et al*. were able to demonstrate that the removal of any one of the constituent oxides resulted in the failure of the system to form a single-phase structure at high temperatures (Figure 7). Interestingly, in the case of the rocksalt system, even removing constituent oxides which induce the enthalpic energy penalty of the phase transformation (i.e. ZnO and CuO) resulted in the formation of a multi-phase structure. This observation suggests that the entropic contribution of adding the fifth component (i.e. $1.61R > 1.39R$) is significant enough to overcome even the energy penalty of the phase transformation. As a result, this method provides strong additional support for the argument of entropy-stabilization of the single-phase structure.

Similar results have been achieved for the perovskite system, as Jiang, *et al*. demonstrated that the addition of a fifth component (either Mn or Nb, with all B-site cations subsequently present in 0.2 molar ratios) to the $Sr(Zr_{0.25}Sn_{0.25}Ti_{0.25}Hf_{0.25})O_3$ four-component, medium-entropy oxide stabilized single-phase formation[4].

Collectively, these three experimental techniques may be used to present solid evidence of entropic stabilization of single-phase HEOs. However, as suggested by the data in Table 1, only a handful of articles in the literature have performed such experiments. While each of the papers referenced in Table 1 do provide evidence of a homogenous single-phase structure, not all isolate entropy as the driving force of this transformation. As a result, there is something of a knowledge gap as to how prevalent entropy-stabilization is across different systems of HEOs. Nonetheless, this presents an exciting opportunity for future research.

IV.V Computational Predictions of Entropy-Stabilization

The subsections above have dealt exclusively with experimental evidence of entropy-stabilization of single-phase transformations in HEOs. However, it is important to note that computational models have also been leveraged to predict both the role of entropy-stabilization as well as, more broadly, the stability of the single-phase in general[37,50–55]. These studies have leveraged computational tools including density functional theory (DFT), Ab initio molecular dynamics (AIMD), CALculation of PHAse Diagrams (CALPHAD), and machine learning (ML) / artificial intelligence (AI). Some of these have used the special quasirandom structures (SQS) approach[37] or incorporated genetic algorithms and other advanced sampling techniques[50,51] to explore the vast configurational space inherent to high entropy systems. While they will not be discussed in further detail here, these computational tools represent important approaches for predicting and understanding the stability of HEOs and other high entropy ceramics. It is likely that the field of HEOs, as well as high-entropy materials in general, will continue to benefit from and drive developments in advanced computational approaches.

V. ENTHALPIC CONSIDERATIONS

Hitherto, for the sake of simplicity, we have treated the enthalpic contribution as something of a "black box," encompassing the relatively abstract concept of the energy penalty of the phase transformation. Fundamentally, this energy penalty is associated with the transition into a single-phase lattice from a different equilibrium configuration. For example, in the canonical rocksalt system, CuO and ZnO have enthalpies of formation, since they do not exist as rocksalt structures under bulk equilibrium conditions:

$$\Delta H_f^{CuO,tenorite\rightarrow rocksalt}$$
$$\Delta H_f^{ZnO,wurtzite\rightarrow rocksalt}$$

As stated previously, these formation enthalpies are represented in the complete ΔH_{mix} term in Equation 2. To briefly reiterate from Equation 2, we have the free energy (ΔG_{mix}) defined as the difference between the enthalpy of mixing (ΔH_{mix}) and the product of the entropy of mixing and temperature ($T\Delta S_{mix}$). We reaffirm two key points: that the second (entropy) term contains a temperature dependence and that ΔG_{mix} must be less than zero for single-phase stabilization, which, assuming a positive ΔH_{mix}, implies the need for a higher magnitude of the $T\Delta S_{mix}$ term. Here, we provide a more in-depth treatment of enthalpy contributions in these HEO systems.

From Equation 2, we have that a single-phase (abbreviated "SP") solid solution is stable relative to its pure components according to the following:

$$\Delta G_{mix}^{SP} < 0 \qquad Eq. 3$$

Assuming ΔH_{mix}^{SP} is positive, this may be written as:

$$\Delta H_{mix}^{SP} < T\Delta S_{mix}^{SP} \qquad Eq. 4$$

Equation 4 provides the concise mathematical description of entropy-stabilization; that is, entropy overcoming a positive enthalpy term. When the only contribution to ΔS_{mix}^{SP} is assumed to be due to ideal configurational entropy, we may combine the previous relationship with Equation 1, which yields:

$$\Delta H_{mix}^{SP} < -RT\sum_{i=1}^{N} x_i \ln x_i \qquad Eq. 5$$

However, this only yields the conditions for which a single-phase is stable relative to pure components. For it to be the equilibrium state for a given system, the single-phase must be stable relative to any possible state, i.e.,

$$\Delta G_{mix}^{SP} < \Delta G_{mix}^{MP} \qquad Eq. 6$$

or,

$$\Delta H_{mix}^{SP} + RT\sum_{i=1}^{N} x_i \ln x_i < \Delta H_{mix}^{MP} - T\Delta S_{mix}^{MP} \qquad Eq. 7$$

For the above relationships, the superscript "MP" now indicates a multi-phase mixture, while "SP" denotes the single-phase. After some manipulation it is found that:

$$\Delta H_{mix}^{SP} < \Delta H_{mix}^{MP} + RT\sum_{i=1}^{N} x_i \sum_{j=1}^{n} f_i^j \ln\left(\frac{y_i^j}{x_i}\right) \qquad Eq. 8$$

For Equation 8, n is the number of phases in the system, f_i^j is the fraction of component i that has partitioned to phase j, and y_i^j is the mole fraction of component i in phase j, which is related to x_i and f_i^j:

$$y_i^j = \frac{f_i^j x_i}{\sum_{i=1}^{n} f_i^j x_i} \qquad Eq. 9$$

The second term in Equation 8 is the decrease in configurational entropy associated with the formation of a multi-phase mixture from a single phase. For a single-phase HEO to be stable (i.e., the equilibrium state), the conditions of both Equations 5 and 8 must be satisfied.

Now let's turn our attention to the concept of "entropy stabilization." A single-phase microstructure can be stable relative to the pure components without the entropy contribution, if ΔH_{mix}^{SP} is negative. A single phase is entropy-stabilized relative to the pure components when $T\Delta S_{mix}^{SP} > \Delta H_{mix}^{SP} > 0$; that is, Equation 5 is satisfied and ΔH_{mix}^{SP} is positive. If the single-phase state is the equilibrium state, ΔH_{mix}^{SP} may be negative, but it must be insufficient to stabilize the single-phase alone, implying that the entropic contribution to ΔG_{mix}^{SP} is required to stabilize the single phase relative to a multi-phase mixture, or:

$$\Delta H_{mix}^{SP} > \Delta G_{mix}^{MP} \qquad Eq. 10$$

$$\Delta H_{mix}^{SP} > \Delta H_{mix}^{MP} - T\Delta S_{mix}^{MP} \qquad Eq. 11$$

$$\Delta H_{mix}^{SP} > \Delta H_{mix}^{MP} + RT\sum_{i=1}^{N} x_i \ln x_i + RT\sum_{i=1}^{N} x_i \sum_{j=1}^{n} f_i^j \ln\left(\frac{y_i^j}{x_i}\right) \qquad Eq. 12$$

This expression combined with Equation 8 provide the conditions for entropy-stabilization of a single-phase HEO.

It is also important to consider the effect of minimization of enthalpy on the ability to form an entropy-stabilized multicomponent oxide. For example, studies to-date have primarily focused on examining systems in which at least two parent phases exist amongst the constituent oxides. In these examples, there is an inherent energy penalty of the phase transition, as has been discussed previously; however, if the HEO were designed to contain constituent oxides having the same parent phase structure, this enthalpy of formation of the single-phase HEO could be substantially lower (or negative) in certain systems.

This lowering of the enthalpy of formation could have significant consequences in terms of the relative ability of the system to be entropy-stabilized at intermediate temperatures. By lowering the enthalpic energy barrier of the single-phase transition, the magnitude of $-T\Delta S_{mix}$ required to make the free energy of the transition zero is also lowered, while the ΔS_{mix} contribution from the ideal configurational entropy should remain unchanged. In some of these cases, it may be possible to observe single-phase stabilization of a 4-cation system because, despite lowering the ideal configurational entropy, the decrease in enthalpy may still exceed the entropy decrease.

From an experimental viewpoint, studying phase transitions in HEOs in this sub-class may present more challenges due to the absence of secondary phases which may be more easily distinguished through prominent peaks in an X-ray diffraction pattern. Nonetheless, provided that the diffractometer in question has sufficient resolution, formation of a single-phase HEO should still be observable by examining the relative peak broadening with temperature (i.e. at lower temperatures, broader, possibly asymmetric diffraction peaks reflect the multi-phase structure, with sharpening of peaks occurring with increasing temperature).

This sub-class of HEOs produced from constituent oxides possessing the same parent phase structure presents an interesting and novel research opportunity. In general, an entropic stabilization to single HEO phase formation would be most readily achieved by combining isostructure oxide components with similar oxidation state and ionic radii [3,10,28]. As described above, the lowering of phase transition enthalpy barrier implies that the temperature required for entropy-stabilization of the single-phase is likewise suppressed, meaning that these phase transformations are more apt to be easily studied in an experimental context. This also suggests that these kinds of systems may also be both the more prevalent examples of true ESOs as well as more relevant in the context of applications. Therefore, considering this approach in future HEO design may yield interesting results on previously unexplored systems.

VI. Considerations Outside the Realm of Ideal Configurational Entropy

As discussed in Section II.II, ESOs represent a special sub-class of HEOs; that is, not all transitions to single-phase HEOs are entropy-stabilized via an ideal configurational entropy[10–12]. The other candidate methods which may drive stabilization deal with short and long-range atomic interactions which vary based on the system[10,12]. The entropy-stabilization argument assumes an ideal configurational entropy for the system as shown in Figure 1; however, localized distortions and unique chemical ordering may cause the system entropy to be lowered, possibly below the threshold necessary for true entropy stabilization. As a result, other atomic-scale forces may drive single-phase transformations in HEOs when the entropy is insufficient. Further analysis of these other thermodynamic considerations is also available in the literature[12].

VI.I Single-Phase Degradation

Previously, we have considered the role of entropy-stabilization as a temperature-dependent process. An interesting reverse effect, in which a temperature increase results in the precipitation of secondary phases from a single-phase structure, has been observed in some HEO systems[4,29]. Based on our prior treatment of entropy-stabilization, such an event is counterintuitive[10], as the magnitude of the $-T\Delta S_{mix}$ term should only increase with temperature. This suggests that there are other competing factors that de-stabilize the single-phase above a temperature threshold. One possible explanation of these observations could be that kinetic factors, such as a temperature-activated diffusion process which causes localized ordering and a decrease in configurational entropy, result in single-phase destabilization.

It should be noted that a single-phase state can be entropy-stabilized at an intermediate temperature but be unstable relative to a multi-phase mixture at elevated temperatures, despite the continuous increase in the configurational entropy contribution to the Gibbs free energy. The peritectoid reaction, $\alpha + \beta \leftrightarrow \gamma$, is a prime example of such a situation. At high temperature the two-phase mixture of $\alpha + \beta$ is the equilibrium state, but as temperature decreases, single-phase γ becomes the equilibrium state. This type of reaction typically occurs when one of the high temperature phases has a significantly higher entropy term that the low temperature phase, for instance, a disordered solid solution compared to an ordered phase (or liquid compared to solid for a peritectic reaction). The disordered phase has a much larger configurational entropy than the ordered phase, allowing the free energy of a two-phase mixture to become stable relative to a single phase.

VI.II Preferential Short- and Long-Range Ordering and Localized Coordination Polyhedra Distortions

As described eloquently by McCormack and Navrotsky[12], any crystal chemical effect that moves the system from an ideal mixing scenario can impact the thermodynamic stability of a HEO. There are a wide variety of crystal-chemical effects known to induce short- and long-range ordering of atoms in complex oxides. Any one of these is a potential cause of single-phase stabilization in HEOs in lieu of ideal entropic stabilization.

Some localized lattice distortions, in particular the Jahn-Teller Effect, have been indicated to likely exist in different HEOs through a combination of experimental and computational studies[37,44,48,50,52,56]. These Jahn-Teller effects — axial elongations or compressions of cation coordination geometries due to degenerative electron states — are significant localized distortions of the lattice which may lead to short-range preferential ordering of the single-phase. These distortions are some of the most evident in the literature on HEOs (Figure 9).

Consider a cation coordination polyhedron in an HEO lattice structure which experiences a Jahn-Teller elongation or compression, as is common for a variety of transition metals in octahedral coordination. The resultant lattice distortion may provide a neighboring cation site with a geometry that is more favorable for a particular species. Therefore, such distortions can produce localized preferential ordering while still maintaining the overall single-phase structure.

Moreover, recent work has shown that some lattice distortions and unique local coordination environments may be energetically favorable in certain systems[37]. This has

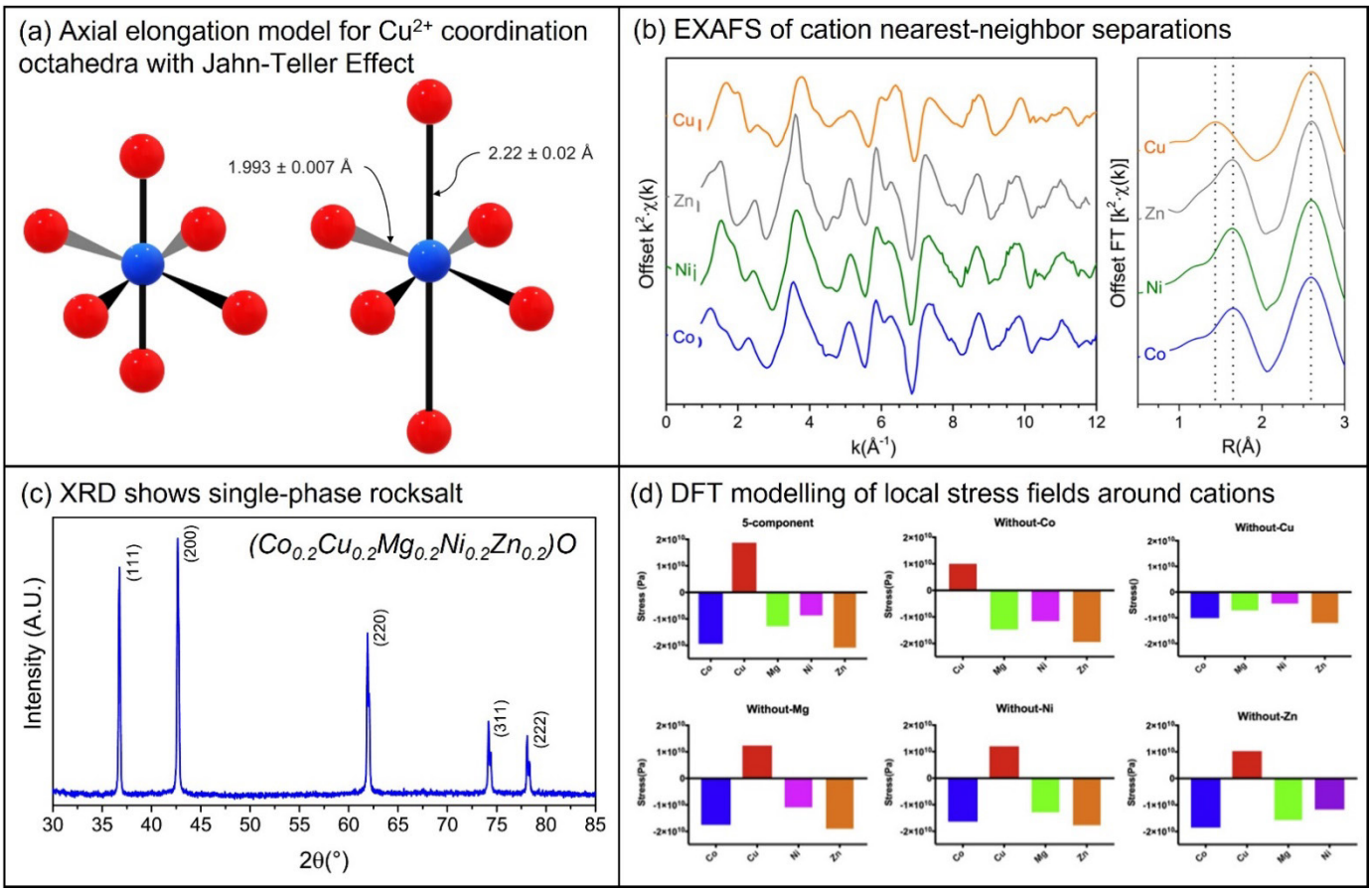

Figure 8. This panel provides examples of localized disorder in the $(Co_{0.2}Cu_{0.2}Mg_{0.2}Ni_{0.2}Zn_{0.2})O$ ESO. (a) Jahn-Teller distortions in Cu-coordination octahedra induce bond distortions[48]. (b) EXAFS data demonstrates variation in the nearest neighbor anion coordination shells unique to the Cu atoms[48]. (c) XRD confirms a single-phase structure, indicating that there must be long-range compensation of short-range distortions in order to observe a uniform lattice parameter[48]. (d) DFT is useful for modelling local lattice distortions induced by these distortions[50].

significant ramifications for phase transformation thermodynamics, as this could lower the energy barrier of the single-phase transformation in multicomponent HEOs. Therefore, short-range preferential ordering within the HEO crystalline lattice could represent a non-trivial factor when considering the relative stability of a given single-phase and could likewise be useful when considering future HEO design.

It is important to note that Jahn-Teller distortions represent only one type of localized order/disorder effect that can impact the propensity for short-range or long-range order and thus single-phase stability. As observed in many complex oxide systems and solid solutions, similar effects can be induced by specific atomic radius-ratios, by charge, spin, or orbital ordering preferences of participating cations, by the presence of cation or anion vacancies, by steric effects such as those induced by lone-pair cations, and many others. There are multiple reports uncovering such effects in HEO systems to date. For example, several studies have examined the effect of variability in ionic radii as it relates to likelihood of single-phase formation. Interestingly, Spiridigliozzi, *et al.*[57] report that producing stable fluorite single-phase HEOs was correlated with a higher standard deviation of cationic size ratios, suggesting that severe lattice distortion directly contributes to the stability of these HEOs. Moreover, Wright, *et al.*[58] observed that reduced thermal conductivity is correlated to the size disparity among cations participating in single-phase medium and high-entropy pyrochlore compositions.

A wide array of ordered to disordered magnetic properties observed in HEO systems to date suggest the influence of cation sublattice order/disorder on resulting physical properties[59]. The class of spinel HEOs has provided several interesting case studies, specifically as related to tetrahedral and octahedral site preferences of specific cation species/oxidation states[18,38].

Recently, a robust characterization effort was undertaken to demonstrate that preferential cation site occupation in the spinel HEO composition $(Co_{0.2}Cr_{0.2}Fe_{0.2}Mn_{0.2}Ni_{0.2})_3O_4$ results from entropic stabilization through maximization of crystal field stabilization effects. The local order significantly departs from an entropy-driven non-preferential arrangement of cations in the lattice[38].

Still other reports have demonstrated that participation or removal of a single specific cation can change HEO phase stability and impact HEO phase selection. For example, Djenadic *et al.*[25] demonstrated that defect fluorite ($MO_{2-\delta}$) HEOs containing equiatomic combinations of Y, La, Ce, Pr, Sm, Nd, and Gd are formed as phase pure compounds when Ce is present, but are synthesized with secondary phases otherwise.

The Ce^{4+} oxidation state and its preferred local bonding environment apparently stabilize a high entropy configuration of RE^{3+} cations in the lattice.

While studies into the exact mechanisms and prevalence of the above cases are still in their infancy, early observations are building a picture that phase stability and phase selection in HEOs may prove to be highly specific to candidate chemical compositions and candidate crystal classes. Local distortions, chemical variations, and configurational preferences like those mentioned above (and their corresponding relative entropic and enthalpic contributions to phase stability) are likely to play key roles in numerous HEO families. Complicating matters, there are tremendous experimental challenges associated with determining the specific site preferences, cation-specific local distortions, and the extent of chemical short range order in HEOs based on complex and even simple oxide archetypes, and consequently, relatively few studies have probed such effects in substantial detail[37,38,46]. To what extent entropic verses enthalpic experimental levers can be used as effective structure-property tuning parameters in various classes of HEOs remains a wide-open research question.

VI.III Metastable Systems

It is possible that certain observed single-phase HEO systems are not in thermodynamic equilibrium but are in fact only metastable states. In such cases, the local to long-range atomic structure features and degree of configurational disorder for a given HEO composition could be highly influenced by the synthesis approach and material processing conditions. It has been observed that various kinetically driven reaction routes, including mechanochemistry, polymeric steric entrapment, and chemical co-precipitation, can be applied to form new (sometimes nanostructured) HEOs, or to lower the temperature of formation of a single phase. In some cases, HEO compositions synthesized by these methods may not be successfully made with conventional solid-state methods, lending support to the idea that at least some compositions may be metastable. At the nanoscale, surface energies of various nanomaterial facets and morphologies will impact the stability of oxide polymorphs and solubility limits for individual components in HEOs[12]. It should be possible to stabilize nanostructured HEO compositions and by extension novel properties that are not readily realized via traditional (high temperature) solid state reaction routes. It has been discussed that sluggish diffusion is a core effect in high-entropy alloys[60]. Should this concept be extended to high-entropy oxides, slow diffusion could make distinguishing thermodynamic equilibrium from metastability more difficult. This places additional significance on verifying the thermodynamic stability of HEO single phases.

VI.IV Non-Ideal Entropy Stabilization

As noted in Voskanyan, *et al*., entropy stabilization may occur outside of the realm of "high-entropy" as has been conventionally defined[32]. In general, the ceramics community has focused attention on entropy-stabilized oxides on complex systems with five or more constituent cations, but that does not preclude entropy-stabilization from being observed in systems with lower ideal configurational entropy or in systems with fewer components. In fact, entropy-stabilization of the single-phase transition has been observed in systems which do not meet the traditional requirements to be classified as "high-entropy," generally due to not meeting the $S_{conf} \geq 1.5R$ threshold[9].

VI.V Cocktail Effects

It is important to note that the interesting properties of multi-constituent cation systems may arise independently from entropy-stabilization, that is, via the cocktail effect. While first proposed for high-entropy alloys[60,61], the cocktail effect may be expanded to high-entropy oxides. Fundamentally, this principle aims to describe the property effects of the complex system as representative of the constituents. While this is a fairly logical and straightforward core effect, it is significant in that it reasserts that, due to the high degree of compositional variability inherent in high-entropy systems, there are a wide range of property spaces that may be accessed. To that end, while certain systems may not be stabilized by ideal configurational entropy as elaborated previously, these systems may still be of significant interest due to cocktail effects arising from the variety of constituent species.

VI.VI Sluggish Diffusion

Additionally, we note that high-entropy systems, due to their high degree of compositional complexity, also experience slow kinetics (i.e. "sluggish diffusion"). This feature is well-documented within the high-entropy alloy community[60], and recent studies contain suggestions that the same is true for high-entropy oxides[8]. For example, as shown in Figure 5a, precipitation of a secondary phase below the critical transition temperature of a pyrochlore ESO as synthesized by Vayer, *et al.*[8] took up to six days at 1400 °C. Such comparatively long time scales, relative to normal ceramic synthesis processes to reach thermodynamic equilibrium is suggestive of such sluggish diffusion effects. This poses a non-trivial experimental challenge, as assessing thermodynamics of many of these phase transformations in HEOs may be significantly hindered by the slow diffusion kinetics of these complex systems. This is an important consideration when conducting temperature-dependent reversibility studies, and in general when considering thermodynamics of high-entropy oxide systems. In such cases, the diffusion kinetics may be so slow that it becomes difficult to study these phase transitions, or at minimum requires substantial time scales for equilibration even at high temperatures.

VII. Synergistic Entropic Effects in HEOs

A number of recent reviews provide summaries and perspectives on the many and possible applications of HEOs and ESOs, including in lithium-ion batteries, chemical catalysis, magnetic materials, dielectrics, etc[11,45,46,62–68]. On a fundamental level, the unique properties of HEOs arise from their unique structural configurations and the contributions of their multiple components. Sarkar et al. have proposed categorizing HEO properties that are due to the interplay of the multiple incorporated elements as 'synergistic,' and those driven by the incorporation of a specific functional element as 'single element driven'[10]. While both categories represent

important and expansive opportunity space, discussion is limited herein to those synergistic properties directly impacted by the potential high entropic stability of HEO compositions. As earlier discussed, entropy is optimized under ideal mixing scenarios. Such a driving force provides a means to optimize properties that benefit from high chemical disorder and configurational complexity. Examples include low thermal conductivity induced by the resulting multiphonon scattering, and highly temperature-stable catalytic, electrochemical, etc. cycling abilities induced by the resulting sluggish diffusion dynamics. Even in cases where entropy is not responsible for phase stabilization, the high configurational entropy inherent in these oxides can lead to important properties which may be exploited in a variety of applications. As a result, simply the presence of high-configurational entropy and multiple components is sufficient to produce interesting and research-worthy properties, even if the HEO is not considered a true "entropy-stabilized" oxide with respect to the phase transformation. Finally, there are a few categories where the entropy-stabilized phase transformation of the compound may itself be of specific functional interest. Highly stable and reversible phase transformations inherent to the subset of ESOs may conceivably be applied in various "phase change material" (PCM)[69] phenomena, including those employed in calorimetric, magnetocaloric, energy storage, data storage, thermal energy harvesting, and many other technologies (though we are unaware of reports of such phenomena in ESO systems to date).

VIII. Future Directions and Outlook

The current status of research into high-entropy oxides presents a plethora of opportunities for future work. Multicomponent, high-entropy oxide systems exhibit promise for use in a wide variety of potential applications, making them an attractive class of novel materials. As a result, understanding how these systems behave thermodynamically is fundamental to designing novel, stable HEOs. Below, we have distilled the discussion of the role of entropy and the thermodynamics of single-phase transformations in HEOs down to a few key takeaway points:

1.) Entropy-stabilized oxides (ESOs) and high-entropy oxides (HEOs) are not interchangeable terms; ESOs refer specifically to systems whose single-phase structures are stabilized through high configurational entropy, while HEOs more generally refer to any systems which have a high configurational entropy but which are not necessarily stabilized by this entropy (summarized in Figure 9).
2.) Entropy-maximization considers an ideal mixing scenario which is impacted by both entropic and enthalpic contributions. As a result, entropy-stabilization is not the only method through which the single-phase transformation in HEOs is driven thermodynamically.
3.) Entropy-stabilization of the phase transformation may be confirmed through a series of corroborating experiments: temperature-dependent reversibility, endothermicity, and component addition.
4.) Few studies have conclusively examined the thermodynamics of phase transformations in high-entropy oxides; as a result, it is difficult to know the true number of HEO systems which experience entropy-stabilization.
5.) Research into thermodynamics of HEOs is still in its infancy, meaning that numerous opportunities exist for future characterization of these oxides. Understanding the thermodynamic stability of these unique systems will aid in the future design of next-generation HEOs with tailored structures and properties.

At present, predicting entropic stabilization in multicomponent ceramics remains difficult, both due to the inherent complexity of these systems and the relatively small body of research completed to date in this field. The characterization tools and experimental methods exist to study entropy-stabilization in HEOs, while the potential compositional and configurational landscape represented among feasible crystal structure classes are simply enormous. It is our hope the above fundamental tenets of the phase transformations in HEOs will help to refine the scientific discourse and assist in streamlining future experimentation.

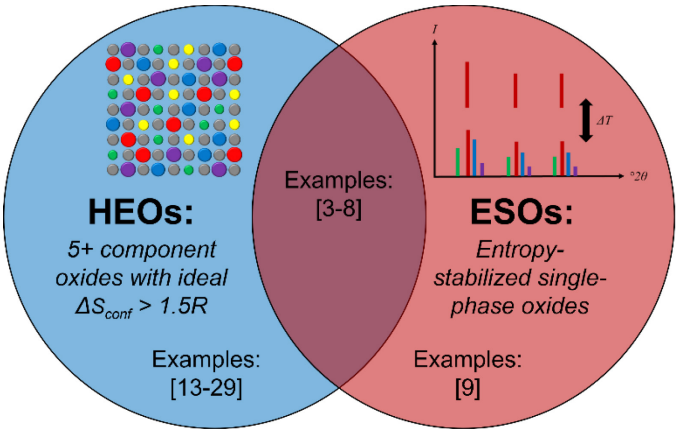

Figure 9. This Venn diagram presents the differences between conventional high-entropy oxides and entropy-stabilized oxides as well as how a number of representative literature examples may be categorized.

IX. Conclusions

A detailed understanding of phase transitions and underlying thermodynamic principles in HEOs is critical to their future design and development. This review has discussed the role of entropy as a driving force which stabilizes single-phase transformations in high-entropy oxides. Additionally, the competing enthalpic driving force and other conditions for single-phase stabilization in high-entropy oxides have been discussed. We have provided the mathematical foundation of the thermodynamics which govern the phase transition and described each of these driving forces. Furthermore, we have reviewed experimental studies which have investigated phase transformations in high-entropy oxides, paying particular attention to the methods used to confirm single-phase formation and to identify the driving force responsible for this phase

transformation. We have also addressed possible considerations for methods of thermodynamic phase-stabilization in HEOs outside of high configurational entropy. Moreover, we discussed the impact of entropy on properties of high-entropy oxides beyond its stabilization of multi-to-single-phase transformations. Finally, we have concluded our discussion with a perspective on the future directions and outlook of studies of high-entropy oxides as they relate to examining phase transformations in these novel materials.

APPENDIX

This work deals primarily with entropy-stabilization and thermodynamic studies of high-entropy oxides; however, there are numerous examples of other high-entropy ceramics, including borides[70], carbides[71–74], and nitrides[75]. These materials have received further interest within the ceramics research community based on many similar concepts. As with high-entropy oxides, the compositional complexity and high-entropy observed in these systems can give rise to unique property spaces of interest across a range of applications. While these materials have not been explicitly discussed here, we refer the reader to additional literature for more targeted insights into this subject matter[45,76].

ACKNOWLEDGEMENTS

RJS was supported by the National Science Foundation Graduate Research Fellowship Program under Grant No. DGE1255832 at the time of submission. KP acknowledges support by the National Science Foundation (DMR-2145174). EAL acknowledges support by the National Science Foundation (DMR-1408722). Any opinions, findings, and conclusions or recommendations expressed in this material are those of the authors and do not necessarily reflect the views of the National Science Foundation. RJS also acknowledges Jon-Paul Maria, George Kotsonis, and Saeed Almishal of Pennsylvania State University for engaging in discussions which assisted in guiding this work.

REFERENCES

(1) Yeh, J.-W.; Chen, S.-K.; Lin, S.-J.; Gan, J.-Y.; Chin, T.-S.; Shun, T.-T.; Tsau, C.-H.; Chang, S.-Y. Nanostructured High-Entropy Alloys with Multiple Principal Elements: Novel Alloy Design Concepts and Outcomes. *Adv Eng Mater* **2004**, *6* (5), 299–303. https://doi.org/10.1002/adem.200300567.

(2) Cantor, B.; Chang, I. T. H.; Knight, P.; Vincent, A. J. B. Microstructural Development in Equiatomic Multicomponent Alloys. *Materials Science and Engineering: A* **2004**, *375–377*, 213–218. https://doi.org/10.1016/j.msea.2003.10.257.

(3) Rost, C. M.; Sachet, E.; Borman, T.; Moballegh, A.; Dickey, E. C.; Hou, D.; Jones, J. L.; Curtarolo, S.; Maria, J.-P. Entropy-Stabilized Oxides. *Nat Commun* **2015**, *6* (1), 8485. https://doi.org/10.1038/ncomms9485.

(4) Jiang, S.; Hu, T.; Gild, J.; Zhou, N.; Nie, J.; Qin, M.; Harrington, T.; Vecchio, K.; Luo, J. A New Class of High-Entropy Perovskite Oxides. *Scripta Materialia* **2018**, *142*, 116–120. https://doi.org/10.1016/j.scriptamat.2017.08.040.

(5) Sarkar, A.; Djenadic, R.; Wang, D.; Hein, C.; Kautenburger, R.; Clemens, O.; Hahn, H. Rare Earth and Transition Metal Based Entropy Stabilised Perovskite Type Oxides. *Journal of the European Ceramic Society* **2018**, *38* (5), 2318–2327. https://doi.org/10.1016/j.jeurceramsoc.2017.12.058.

(6) Chen, K.; Pei, X.; Tang, L.; Cheng, H.; Li, Z.; Li, C.; Zhang, X.; An, L. A Five-Component Entropy-Stabilized Fluorite Oxide. *Journal of the European Ceramic Society* **2018**, *38* (11), 4161–4164. https://doi.org/10.1016/j.jeurceramsoc.2018.04.063.

(7) Spiridigliozzi, L.; Ferone, C.; Cioffi, R.; Accardo, G.; Frattini, D.; Dell'Agli, G. Entropy-Stabilized Oxides Owning Fluorite Structure Obtained by Hydrothermal Treatment. *Materials* **2020**, *13* (3), 558. https://doi.org/10.3390/ma13030558.

(8) Vayer, F.; Decorse, C.; Bérardan, D.; Dragoe, N. New Entropy-Stabilized Oxide with Pyrochlore Structure: Dy2(Ti0.2Zr0.2Hf0.2Ge0.2Sn0.2)2O7. *Journal of Alloys and Compounds* **2021**, *883*, 160773. https://doi.org/10.1016/j.jallcom.2021.160773.

(9) Chen, K.; Ma, J.; Wang, H.; Li, C.; An, L. Entropy-Stabilized Oxides with Medium Configurational Entropy. *Ceramics International* **2021**, *47* (7), 9979–9983. https://doi.org/10.1016/j.ceramint.2020.12.143.

(10) Sarkar, A.; Breitung, B.; Hahn, H. High Entropy Oxides: The Role of Entropy, Enthalpy and Synergy. *Scripta Materialia* **2020**, *187*, 43–48. https://doi.org/10.1016/j.scriptamat.2020.05.019.

(11) Sarkar, A.; Wang, Q.; Schiele, A.; Chellali, M. R.; Bhattacharya, S. S.; Wang, D.; Brezesinski, T.; Hahn, H.; Velasco, L.; Breitung, B. High-Entropy Oxides: Fundamental Aspects and Electrochemical Properties. *Adv Mater* **2019**, *31* (26), 1806236. https://doi.org/10.1002/adma.201806236.

(12) McCormack, S. J.; Navrotsky, A. Thermodynamics of High Entropy Oxides. *Acta Materialia* **2021**, *202*, 1–21. https://doi.org/10.1016/j.actamat.2020.10.043.

(13) Dąbrowa, J.; Stygar, M.; Mikuła, A.; Knapik, A.; Mroczka, K.; Tejchman, W.; Danielewski, M.; Martin, M. Synthesis and Microstructure of the (Co,Cr,Fe,Mn,Ni) 3 O 4 High Entropy Oxide Characterized by Spinel Structure. *Materials Letters* **2018**, *216*, 32–36. https://doi.org/10.1016/j.matlet.2017.12.148.

(14) Mao, A.; Xiang, H.-Z.; Zhang, Z.-G.; Kuramoto, K.; Zhang, H.; Jia, Y. A New Class of Spinel High-Entropy Oxides with Controllable Magnetic Properties. *Journal of Magnetism and Magnetic Materials* **2020**, *497*, 165884. https://doi.org/10.1016/j.jmmm.2019.165884.

(15) Tseng, K.-P.; Yang, Q.; McCormack, S. J.; Kriven, W. M. High-entropy, Phase-constrained, Lanthanide Sesquioxide. *J Am Ceram Soc* **2020**, *103* (1), 569–576. https://doi.org/10.1111/jace.16689.

(16) Gild, J.; Samiee, M.; Braun, J. L.; Harrington, T.; Vega, H.; Hopkins, P. E.; Vecchio, K.; Luo, J. High-Entropy Fluorite Oxides. *Journal of the European Ceramic*

Society **2018**, *38* (10), 3578–3584. https://doi.org/10.1016/j.jeurceramsoc.2018.04.010.

(17) Cardoso, A. L. F.; Perdomo, C. P. F.; Kiminami, R. H. G. A.; Gunnewiek, R. F. K. Enhancing the Stabilization of Nanostructured Rocksalt-like High Entropy Oxide by Gd Addition. *Materials Letters* **2021**, *285*, 129175. https://doi.org/10.1016/j.matlet.2020.129175.

(18) Musicó, B.; Wright, Q.; Ward, T. Z.; Grutter, A.; Arenholz, E.; Gilbert, D.; Mandrus, D.; Keppens, V. Tunable Magnetic Ordering through Cation Selection in Entropic Spinel Oxides. *Phys. Rev. Materials* **2019**, *3* (10), 104416. https://doi.org/10.1103/PhysRevMaterials.3.104416.

(19) Stygar, M.; Dąbrowa, J.; Moździerz, M.; Zajusz, M.; Skubida, W.; Mroczka, K.; Berent, K.; Świerczek, K.; Danielewski, M. Formation and Properties of High Entropy Oxides in Co-Cr-Fe-Mg-Mn-Ni-O System: Novel (Cr,Fe,Mg,Mn,Ni)3O4 and (Co,Cr,Fe,Mg,Mn)3O4 High Entropy Spinels. *Journal of the European Ceramic Society* **2020**, *40* (4), 1644–1650. https://doi.org/10.1016/j.jeurceramsoc.2019.11.030.

(20) Teng, Z.; Zhu, L.; Tan, Y.; Zeng, S.; Xia, Y.; Wang, Y.; Zhang, H. Synthesis and Structures of High-Entropy Pyrochlore Oxides. *Journal of the European Ceramic Society* **2020**, *40* (4), 1639–1643. https://doi.org/10.1016/j.jeurceramsoc.2019.12.008.

(21) Teng, Z.; Tan, Y.; Zeng, S.; Meng, Y.; Chen, C.; Han, X.; Zhang, H. Preparation and Phase Evolution of High-Entropy Oxides A2B2O7 with Multiple Elements at A and B Sites. *Journal of the European Ceramic Society* **2021**, *41* (6), 3614–3620. https://doi.org/10.1016/j.jeurceramsoc.2021.01.013.

(22) Karthick, G.; Raman, L.; Murty, B. S. Phase Evolution and Mechanical Properties of Novel Nanocrystalline Y2(TiZrHfMoV)2O7 High Entropy Pyrochlore. *J Mater Sci Technol* **2021**, *82*, 214–226. https://doi.org/10.1016/j.jmst.2020.12.025.

(23) Vinnik, D. A.; Trofimov, E. A.; Zhivulin, V. E.; Zaitseva, O. V.; Gudkova, S. A.; Starikov, A. Yu.; Zherebtsov, D. A.; Kirsanova, A. A.; Häßner, M.; Niewa, R. High-Entropy Oxide Phases with Magnetoplumbite Structure. *Ceramics International* **2019**, *45* (10), 12942–12948. https://doi.org/10.1016/j.ceramint.2019.03.221.

(24) Mao, A.; Xie, H.-X.; Xiang, H.-Z.; Zhang, Z.-G.; Zhang, H.; Ran, S. A Novel Six-Component Spinel-Structure High-Entropy Oxide with Ferrimagnetic Property. *Journal of Magnetism and Magnetic Materials* **2020**, *503*, 166594. https://doi.org/10.1016/j.jmmm.2020.166594.

(25) Djenadic, R.; Sarkar, A.; Clemens, O.; Loho, C.; Botros, M.; Chakravadhanula, V. S. K.; Kübel, C.; Bhattacharya, S. S.; Gandhi, A. S.; Hahn, H. Multicomponent Equiatomic Rare Earth Oxides. *Materials Research Letters* **2017**, *5* (2), 102–109. https://doi.org/10.1080/21663831.2016.1220433.

(26) Sharma, Y.; Musico, B. L.; Gao, X.; Hua, C.; May, A. F.; Herklotz, A.; Rastogi, A.; Mandrus, D.; Yan, J.; Lee, H. N.; Chisholm, M. F.; Keppens, V.; Ward, T. Z. Single-Crystal High Entropy Perovskite Oxide Epitaxial Films. *Phys. Rev. Materials* **2018**, *2* (6), 060404. https://doi.org/10.1103/PhysRevMaterials.2.060404.

(27) Braun, J. L.; Rost, C. M.; Lim, M.; Giri, A.; Olson, D. H.; Kotsonis, G. N.; Stan, G.; Brenner, D. W.; Maria, J.-P.; Hopkins, P. E. Charge-Induced Disorder Controls the Thermal Conductivity of Entropy-Stabilized Oxides. *Adv Mater* **2018**, *30* (51), 1805004. https://doi.org/10.1002/adma.201805004.

(28) Sarkar, A.; Djenadic, R.; Usharani, N. J.; Sanghvi, K. P.; Chakravadhanula, V. S. K.; Gandhi, A. S.; Hahn, H.; Bhattacharya, S. S. Nanocrystalline Multicomponent Entropy Stabilised Transition Metal Oxides. *Journal of the European Ceramic Society* **2017**, *37* (2), 747–754. https://doi.org/10.1016/j.jeurceramsoc.2016.09.018.

(29) Zhou, S.; Pu, Y.; Zhang, Q.; Shi, R.; Guo, X.; Wang, W.; Ji, J.; Wei, T.; Ouyang, T. Microstructure and Dielectric Properties of High Entropy Ba(Zr0.2Ti0.2Sn0.2Hf0.2Me0.2)O3 Perovskite Oxides. *Ceramics International* **2020**, *46* (6), 7430–7437. https://doi.org/10.1016/j.ceramint.2019.11.239.

(30) Jothi, P. R.; Liyanage, W.; Jiang, B.; Paladugu, S.; Olds, D.; Gilbert, D.; Page, K. Persistent Structure and Frustrated Magnetism in High Entropy Rare-Earth Zirconates. *Small* **2022**, *18* (5), 2101323. https://doi.org/10.1002/smll.202101323.

(31) McCormack, S. J.; Kriven, W. M. Crystal Structure Solution for the A6B2O17 (A = Zr, Hf; B = Nb, Ta) Superstructure. *Acta Cryst* **2019**, *75*, 227–234. https://doi.org/10.1107/S2052520619001963.

(32) Voskanyan, A. A.; Lilova, K.; McCormack, S. J.; Kriven, W. M.; Navrotsky, A. A New Class of Entropy Stabilized Oxides: Commensurately Modulated A6B2O17 (A = Zr, Hf; B = Nb, Ta) Structures. *Scripta Materialia* **2021**, *204*, 114139. https://doi.org/10.1016/j.scriptamat.2021.114139.

(33) Antao, S. M. Crystal Structure of an Anisotropic Pyrope Garnet That Contains Two Cubic Phases. *Minerals* **2021**, *11* (12), 1320. https://doi.org/10.3390/min11121320.

(34) Antao, S. M. Three Cubic Phases Intergrown in a Birefringent Andradite-Grossular Garnet and Their Implications. *Phys Chem Minerals* **2013**, *40* (9), 705–716. https://doi.org/10.1007/s00269-013-0606-4.

(35) Antao, S. M. The Mystery of Birefringent Garnet: Is the Symmetry Lower than Cubic? *Powder Diffr* **2013**, *28* (4), 281–288. https://doi.org/10.1017/S0885715613000523.

(36) Kemei, M. C.; Harada, J. K.; Seshadri, R.; Suchomel, M. R. Structural Change and Phase Coexistence upon Magnetic Ordering in the Magnetodielectric Spinel Mn3O4. *Phys Rev B* **2014**, *90*, 064418. https://doi.org/10.1103/PhysRevB.90.064418.

(37) Jiang, B.; Bridges, C. A.; Unocic, R. R.; Pitike, K. C.; Cooper, V. R.; Zhang, Y.; Lin, D.-Y.; Page, K. Probing the Local Site Disorder and Distortion in Pyrochlore High-Entropy Oxides. *J. Am. Chem. Soc.* **2021**, *143* (11), 4193–4204. https://doi.org/10.1021/jacs.0c10739.

(38) Sarkar, A.; Eggert, B.; Witte, R.; Lill, J.; Velasco, L.; Wang, Q.; Sonar, J.; Ollefs, K.; Bhattacharya, S. S.; Brand, R. A.; Wende, H.; de Groot, F. M. F.; Clemens, O.; Hahn, H.; Kruk, R. Comprehensive Investigation of Crystallographic, Spin-Electronic and Magnetic Structure of (Co0.2Cr0.2Fe0.2Mn0.2Ni0.2)3O4: Unraveling the Suppression of Configuration Entropy in High Entropy Oxides. *Acta Mater* **2022**, *226*, 117581. https://doi.org/10.1016/j.actamat.2021.117581.

(39) Zhang, J.; Yan, J.; Calder, S.; Zheng, Q.; McGuire, M. A.; Abernathy, D. L.; Ren, Y.; Lapidus, S. H.; Page, K.; Zheng, H.; Freeland, J. W.; Budai, J. D.; Hermann, R. P. Long-Range Antiferromagnetic Order in a Rocksalt High Entropy Oxide. *Chem. Mater.* **2019**, *31* (10), 3705–3711. https://doi.org/10.1021/acs.chemmater.9b00624.

(40) Zhu, H.; Xie, H.; Zhao, Y.; Dai, S.; Li, M.; Wang, X. Structure and Magnetic Properties of a Class of Spinel High-Entropy Oxides. *Journal of Magnetism and Magnetic Materials* **2021**, *535*, 168063. https://doi.org/10.1016/j.jmmm.2021.168063.

(41) Xiang, H.-Z.; Xie, H.-X.; Chen, Y.-X.; Zhang, H.; Mao, A.; Zheng, C.-H. Porous Spinel-Type (Al0.2CoCrFeMnNi)0.58O4-δ High-Entropy Oxide as a Novel High-Performance Anode Material for Lithium-Ion Batteries. *J Mater Sci* **2021**, *56*, 8127–8142. https://doi.org/10.1007/s10853-021-05805-5.

(42) Parida, T.; Karati, A.; Guruvidyathri, K.; Murty, B. S.; Markandeyulu, G. Novel Rare-Earth and Transition Metal-Based Entropy Stabilized Oxides with Spinel Structure. *Scripta Materialia* **2020**, *178*, 513–517. https://doi.org/10.1016/j.scriptamat.2019.12.027.

(43) Mao, A.; Quan, F.; Xiang, H.-Z.; Zhang, Z.-G.; Kuramoto, K.; Xia, A.-L. Facile Synthesis and Ferrimagnetic Property of Spinel (CoCrFeMnNi)3O4 High-Entropy Oxide Nanocrystalline Powder. *J Mol Struct* **2019**, *1194*, 11–18. https://doi.org/10.1016/j.molstruc.2019.05.073.

(44) Berardan, D.; Meena, A. K.; Franger, S.; Herrero, C.; Dragoe, N. Controlled Jahn-Teller Distortion in (MgCoNiCuZn)O-Based High Entropy Oxides. *Journal of Alloys and Compounds* **2017**, *704*, 693–700. https://doi.org/10.1016/j.jallcom.2017.02.070.

(45) Oses, C.; Toher, C.; Curtarolo, S. High-Entropy Ceramics. *Nat Rev Mater* **2020**, *5*, 295–309. https://doi.org/10.1038/s41578-019-0170-8.

(46) Musicó, B. L.; Gilbert, D.; Ward, T. Z.; Page, K.; George, E.; Yan, J.; Mandrus, D.; Keppens, V. The Emergent Field of High Entropy Oxides: Design, Prospects, Challenges, and Opportunities for Tailoring Material Properties. *APL Materials* **2020**, *8* (4), 040912. https://doi.org/10.1063/5.0003149.

(47) Chellali, M. R.; Sarkar, A.; Nandam, S. H.; Bhattacharya, S. S.; Breitung, B.; Hahn, H.; Velasco, L. On the Homogeneity of High Entropy Oxides: An Investigation at the Atomic Scale. *Scripta Materialia* **2019**, *166*, 58–63. https://doi.org/10.1016/j.scriptamat.2019.02.039.

(48) Rost, C. M.; Rak, Z.; Brenner, D. W.; Maria, J. Local Structure of the $Mg_x Ni_x Co_x Cu_x Zn_x O$ (x =0.2) Entropy-stabilized Oxide: An EXAFS Study. *J Am Ceram Soc* **2017**, *100* (6), 2732–2738. https://doi.org/10.1111/jace.14756.

(49) Navrotsky, A. Progress and New Directions in Calorimetry: A 2014 Perspective. *J. Am. Ceram. Soc.* **2014**, *97* (11), 3349–3359. https://doi.org/10.1111/jace.13278.

(50) Anand, G.; Wynn, A. P.; Handley, C. M.; Freeman, C. L. Phase Stability and Distortion in High-Entropy Oxides. *Acta Materialia* **2018**, *146*, 119–125. https://doi.org/10.1016/j.actamat.2017.12.037.

(51) Pitike, K. C.; Kc, S.; Eisenbach, M.; Bridges, C. A.; Cooper, V. R. Predicting the Phase Stability of Multicomponent High-Entropy Compounds. *Chem. Mater.* **2020**, *32* (17), 7507–7515. https://doi.org/10.1021/acs.chemmater.0c02702.

(52) Rák, Zs.; Maria, J.-P.; Brenner, D. W. Evidence for Jahn-Teller Compression in the (Mg, Co, Ni, Cu, Zn)O Entropy-Stabilized Oxide: A DFT Study. *Materials Letters* **2018**, *217*, 300–303. https://doi.org/10.1016/j.matlet.2018.01.111.

(53) Rak, Zs.; Rost, C. M.; Lim, M.; Sarker, P.; Toher, C.; Curtarolo, S.; Maria, J.-P.; Brenner, D. W. Charge Compensation and Electrostatic Transferability in Three Entropy-Stabilized Oxides: Results from Density Functional Theory Calculations. *Journal of Applied Physics* **2016**, *120* (9), 095105. https://doi.org/10.1063/1.4962135.

(54) Kaufmann, K.; Maryanovsky, D.; Mellor, W. M.; Zhu, C.; Rosengarten, A. S.; Harrington, T. J.; Oses, C.; Toher, C.; Curtarolo, S.; Vecchio, K. S. Discovery of High-Entropy Ceramics via Machine Learning. *npj Comput Mater* **2020**, *6* (1), 42. https://doi.org/10.1038/s41524-020-0317-6.

(55) Zhong, Y.; Sabarou, H.; Yan, X.; Yang, M.; Gao, M. C.; Liu, X.; Sisson, Jr, R. D. Exploration of High Entropy Ceramics (HECs) with Computational Thermodynamics - A Case Study with LaMnO3±δ. *Mater Des* **2019**, *182*, 108060. https://doi.org/10.1016/j.matdes.2019.108060.

(56) Sushil, J.; Kumar, A.; Gautam, A.; Ahmad, M. I. High Entropy Phase Evolution and Fine Structure of Five Component Oxide (Mg, Co, Ni, Cu, Zn)O by Citrate Gel Method. *Materials Chemistry and Physics* **2021**, *259*, 124014. https://doi.org/10.1016/j.matchemphys.2020.124014.

(57) Spiridigliozzi, L.; Ferone, C.; Cioffi, R.; Dell'Agli, G. A Simple and Effective Predictor to Design Novel Fluorite-Structured High Entropy Oxides (HEOs). *Acta Materialia* **2021**, *202*, 181–189. https://doi.org/10.1016/j.actamat.2020.10.061.

(58) Wright, A. J.; Wang, Q.; Ko, S.-T.; Chung, K. M.; Chen, R.; Luo, J. Size Disorder as a Descriptor for Predicting Reduced Thermal Conductivity in Medium- and High-Entropy Pyrochlore Oxides. *Scripta Materialia* **2020**, *181*, 76–81. https://doi.org/10.1016/j.scriptamat.2020.02.011.

(59) Sarkar, A.; Kruk, R.; Hahn, H. Magnetic Properties of High Entropy Oxides. *Dalton Trans.* **2021**, *50* (6), 1973–1982. https://doi.org/10.1039/D0DT04154H.

(60) Miracle, D. B.; Senkov, O. N. A Critical Review of High Entropy Alloys and Related Concepts. *Acta Mater* **2017**, *122*, 448–511. https://doi.org/10.1016/j.actamat.2016.08.081.

(61) Ranganathan, S. Alloyed Pleasures: Multimetallic Cocktails. *CURRENT SCIENCE* **2003**, *85* (10), 3.

(62) Zhang, R.-Z.; Reece, M. J. Review of High Entropy Ceramics: Design, Synthesis, Structure and Properties. *J. Mater. Chem. A* **2019**, *7* (39), 22148–22162. https://doi.org/10.1039/C9TA05698J.

(63) Sarkar, A.; Velasco, L.; Wang, D.; Wang, Q.; Talasila, G.; de Biasi, L.; Kübel, C.; Brezesinski, T.; Bhattacharya, S. S.; Hahn, H.; Breitung, B. High Entropy Oxides for Reversible Energy Storage. *Nat Commun* **2018**, *9* (1), 3400. https://doi.org/10.1038/s41467-018-05774-5.

(64) Lun, Z.; Ouyang, B.; Kwon, D.-H.; Ha, Y.; Foley, E. E.; Huang, T.-Y.; Cai, Z.; Kim, H.; Balasubramanian, M.; Sun, Y.; Huang, J.; Tian, Y.; Kim, H.; McCloskey, B. D.; Yang, W.; Clément, R. J.; Ji, H.; Ceder, G. Cation-Disordered Rocksalt-Type High-Entropy Cathodes for Li-Ion Batteries. *Nat. Mater.* **2021**, *20* (2), 214–221. https://doi.org/10.1038/s41563-020-00816-0.

(65) Wang, Q.; Sarkar, A.; Li, Z.; Lu, Y.; Velasco, L.; Bhattacharya, S. S.; Brezesinski, T.; Hahn, H.; Breitung, B. High Entropy Oxides as Anode Material for Li-Ion Battery Applications: A Practical Approach. *Electrochemistry Communications* **2019**, *100*, 121–125. https://doi.org/10.1016/j.elecom.2019.02.001.

(66) Albedwawi, S. H.; AlJaberi, A.; Haidemenopoulos, G. N.; Polychronopoulou, K. High Entropy Oxides-Exploring a Paradigm of Promising Catalysts: A Review. *Materials & Design* **2021**, *202*, 109534. https://doi.org/10.1016/j.matdes.2021.109534.

(67) Chen, H.; Fu, J.; Zhang, P.; Peng, H.; Abney, C. W.; Jie, K.; Liu, X.; Chi, M.; Dai, S. Entropy-Stabilized Metal Oxide Solid Solutions as CO Oxidation Catalysts with High-Temperature Stability. *J. Mater. Chem. A* **2018**, *6* (24), 11129–11133. https://doi.org/10.1039/C8TA01772G.

(68) Bérardan, D.; Franger, S.; Dragoe, D.; Meena, A. K.; Dragoe, N. Colossal Dielectric Constant in High Entropy Oxides. *Phys. Status Solidi RRL* **2016**, *10* (4), 328–333. https://doi.org/10.1002/pssr.201600043.

(69) Chen, X.; Tang, Z.; Liu, P.; Gao, H.; Chang, Y.; Wang, G. Smart Utilization of Multifunctional Metal Oxides in Phase Change Materials. *Matter* **2020**, *3* (3), 708–741. https://doi.org/10.1016/j.matt.2020.05.016.

(70) Gild, J.; Zhang, Y.; Harrington, T.; Jiang, S.; Hu, T.; Quinn, M. C.; Mellor, W. M.; Zhou, N.; Vecchio, K.; Luo, J. High-Entropy Metal Diborides: A New Class of High-Entropy Materials and a New Type of Ultrahigh Temperature Ceramics. *Sci Rep* **2016**, *6* (1), 37946. https://doi.org/10.1038/srep37946.

(71) Sarker, P.; Harrington, T.; Toher, C.; Oses, C.; Samiee, M.; Maria, J.-P.; Brenner, D. W.; Vecchio, K. S.; Curtarolo, S. High-Entropy High-Hardness Metal Carbides Discovered by Entropy Descriptors. *Nat Commun* **2018**, *9* (1), 4980. https://doi.org/10.1038/s41467-018-07160-7.

(72) Castle, E.; Csanádi, T.; Grasso, S.; Dusza, J.; Reece, M. Processing and Properties of High-Entropy Ultra-High Temperature Carbides. *Sci Rep* **2018**, *8* (1), 8609. https://doi.org/10.1038/s41598-018-26827-1.

(73) Yan, X.; Constantin, L.; Lu, Y.; Silvain, J.-F.; Nastasi, M.; Cui, B. (Hf0.2Zr0.2Ta0.2Nb0.2Ti0.2)C High-Entropy Ceramics with Low Thermal Conductivity. *Journal of the American Ceramic Society* **2018**, *101* (10), 4486–4491. https://doi.org/10.1111/jace.15779.

(74) Hossain, M. D.; Borman, T.; Oses, C.; Esters, M.; Toher, C.; Feng, L.; Kumar, A.; Fahrenholtz, W. G.; Curtarolo, S.; Brenner, D. W.; LeBeau, J. M.; Maria, J.-P. Entropy Landscaping of High-Entropy Carbides. *Advanced Materials* **2021**, *33* (42), 2102904. https://doi.org/10.1002/adma.202102904.

(75) Jin, T.; Sang, X.; Unocic, R. R.; Kinch, R. T.; Liu, X.; Hu, J.; Liu, H.; Dai, S. Mechanochemical-Assisted Synthesis of High-Entropy Metal Nitride via a Soft Urea Strategy. *Advanced Materials* **2018**, *30* (23), 1707512. https://doi.org/10.1002/adma.201707512.

(76) Toher, C.; Oses, C.; Esters, M.; Hicks, D.; Kotsonis, G. N.; Rost, C. M.; Brenner, D. W.; Maria, J.-P.; Curtarolo, S. High-Entropy Ceramics: Propelling Applications through Disorder. *MRS Bulletin* **2022**, *47* (2), 194–202. https://doi.org/10.1557/s43577-022-00281-x.